Circadian programming of the ellipsoid body sleep homeostat in *Drosophila*

Tomas Andreani[1], Clark Rosensweig[1], Shiju Sisobhan[1], Emmanuel Ogunlana[1], William Kath[2], and Ravi Allada[1,3,*]

[1]Department of Neurobiology, Northwestern University, Evanston, IL, 60208 USA

[2]Department of Engineering Sciences and Applied Mathematics, Northwestern University, Evanston, Illinois 60208

[3]Lead Contact

*Correspondence: r-allada@northwestern.edu

Summary

Homeostatic and circadian processes collaborate to appropriately time and consolidate sleep and wake. To understand how these processes are integrated, we scheduled brief sleep deprivation at different times of day in *Drosophila* and find elevated morning rebound compared to evening. These effects depend on discrete morning and evening clock neurons, independent of their roles in circadian locomotor activity. In the R5 ellipsoid body sleep homeostat, we identified elevated morning expression of activity dependent and presynaptic gene expression as well as the presynaptic protein BRUCHPILOT consistent with regulation by clock circuits. These neurons also display elevated calcium levels in response to sleep loss in the morning, but not the evening consistent with the observed time-dependent sleep rebound. These studies reveal the circuit and molecular mechanisms by which discrete circadian clock neurons program a homeostatic sleep center.

Introduction

The classic two process model posits that the circadian clock and the sleep homeostat independently regulate sleep (Borbely, 1982; Borbely, Daan, Wirz-Justice, & Deboer, 2016). The circadian process, via phased activity changes in central pacemaker neurons, times and consolidates sleep-wake (Patke, Young, & Axelrod, 2020). The less well understood homeostatic process, often assayed after extended sleep deprivation, promotes sleep length, depth, and amount as a function of the duration and intensity of prior waking experience (Deboer & Tobler, 2000; Franken, Dijk, Tobler, & Borbely, 1991; Huber et al., 2004; Werth, Dijk, Achermann, & Borbely, 1996). Sleep homeostasis is thought to be mediated by the accumulation of various wake-dependent factors, such as synaptic strength (Tononi & Cirelli, 2014), which are subsequently dissipated with sleep.

While homeostatic drive persists in the absence of a functioning circadian clock(Tobler, Borbely, & Groos, 1983), homeostatic drive can be modulated by the circadian clock. Abolishing clock output through mutation of most core clock genes (Franken et al., 2006; Laposky et al., 2005; Wisor et al., 2002) or electrolytic ablation of the mammalian circadian pacemaker, the suprachiasmatic nuclei (SCN) (Easton, Meerlo, Bergmann, & Turek, 2004) reduces SD-induced changes in non-rapid eye movement (NREM) sleep, an indicator of homeostatic sleep drive in mammals. As circadian clock genes and even the SCN may regulate processes that are not themselves rhythmic(Fernandez, Nurilov, Feliciano, McDonald, & Simon, 2014), these studies leave open the question about whether homeostasis is circadian regulated. To more definitely address the interaction between the clock and the homeostat, sleep-wake have been scheduled to different circadian times in forced desynchrony protocols(Dijk & Czeisler, 1994, 1995). In one such protocol, sleep and wake are scheduled to occur every 28 hours, allowing the circadian

clock to free-run with a ~24 h period. Under these conditions, a variety of indicators of homeostatic drive such as total time asleep, latency to sleep, and NREM sleep time are reduced in the evening independently of time awake (Dijk & Czeisler, 1994, 1995; Dijk & Duffy, 1999; Lazar, Lazar, & Dijk, 2015), consistent with the idea that the clock sustains wakefulness at the end of the waking period in the evening. Yet the molecular and circuit mechanisms by which the circadian clock modulates sleep homeostasis remain unclear.

To understand the mechanistic basis of circadian regulation of sleep homeostasis, we are using *Drosophila,* a well-established model for investigating the molecular and neural basis of circadian rhythms and sleep. Sleep is characterized by quiescence, increased arousal thresholds, changes in neuronal activity, and circadian and homeostatic regulation(Campbell & Tobler, 1984). Flies display each of these hallmarks (Hendricks et al., 2000; Shaw, Cirelli, Greenspan, & Tononi, 2000; van Alphen, Yap, Kirszenblat, Kottler, & van Swinderen, 2013) and have simple, well characterized circadian and sleep neural networks (Dubowy & Sehgal, 2017; Shafer & Keene, 2021). About 150 central pacemaker neurons that express molecular clocks (Dubowy & Sehgal, 2017). Of these, four small ventral lateral neurons (sLNvs) (per hemisphere) that expressing pigment dispersing factor (PDF) are necessary for driving morning activity in anticipation of lights on and exhibit peak levels of calcium around dawn (~ZT0) (Grima, Chelot, Xia, & Rouyer, 2004; Liang et al., 2019; Liang, Holy, & Taghert, 2017; Stoleru, Peng, Agosto, & Rosbash, 2004). The dorsal lateral neurons (LNds) and a 5th PDF^- sLNv are necessary for evening anticipation of lights off and show a corresponding evening calcium peak (ZT8-ZT10) (Gossan et al., 2014; Grima et al., 2004; Liang et al., 2019; Liang et al., 2017; Stoleru et al., 2004). The posterior DN1 (DN1ps) consist of glutamate-positive (Glu^+) subsets necessary for morning anticipation and Glu^- necessary for evening anticipation under low light conditions

(Chatterjee et al., 2018). Lateral posterior neurons (LPN) are not necessary for anticipation but are uniquely sensitive to temperature cycling (Miyasako, Umezaki, & Tomioka, 2007). Specific pacemaker subsets have been linked to wake promotion (PDF^+ large LNv (Chung, Kilman, Keath, Pitman, & Allada, 2009; Parisky et al., 2008; Sheeba et al., 2008), diuretic hormone 31 ($DH31^+$) DN1ps(Kunst et al., 2014)) and sleep promotion (Glu^+ DN1ps (Guo et al., 2016), Allostatin A^+ LPNs (Ni et al., 2019)), independently of their clock functions. How these neurons regulate homeostatic sleep drive itself remains unsettled.

Timed signaling from these clock neurons converges on the neuropil of the ellipsoid body (EB). The sLNvs and LNds appear to communicate to R5 EB neurons through an intermediate set of dopaminergic PPM3 neurons based largely on correlated calcium oscillations(Liang et al., 2019). The anterior projecting subset of DN1ps provide sleep promoting input to other EB neurons (R2/R4M) via tubercular bulbar (TuBu) interneurons (Guo, Holla, Diaz, & Rosbash, 2018; Lamaze, Kratschmer, Chen, Lowe, & Jepson, 2018). Activation of a subset of these TuBu neurons synchronizes the activity of the R5 neurons which is important for sleep maintenance (Raccuglia et al., 2019). Critically, the R5 neurons are at the core of sleep homeostasis in *Drosophila* (Liu, Liu, Tabuchi, & Wu, 2016). R5 neuronal activity is both necessary and sufficient for sleep rebound (Liu et al., 2016). Extended sleep deprivation (12-24h) elevates calcium, the critical presynaptic protein BRUCHPILOT (BRP), and action potential firing rates in R5 neurons. The changes in BRP in this region not only reflect increased sleep drive following SD but also knockdown (KD) of *brp* in R5 decreases rebound (Huang, Piao, Beuschel, Gotz, & Sigrist, 2020) suggesting it functions directly in regulating sleep homeostasis. R5 neurons stimulate downstream neurons in the dorsal fan-shaped body (dFB), which are sufficient to produce sleep (Donlea, Pimentel, & Miesenbock, 2014; Donlea, Thimgan, Suzuki, Gottschalk, &

Shaw, 2011; Liu et al., 2016). Yet how the activity of key clock neurons are integrated with signals from the R5 homeostat to determine sleep drive remains unclear.

Here we dissect the link between the circadian and homeostatic drives by examining which clock neural circuits regulate sleep rebound at different times of day in *Drosophila*. Akin to the forced desynchrony protocols, we enforced wakefulness at different times of day and assessed sleep rebound. We exposed flies to 7 h cycles of sleep deprivation and recovery, enabling assessment of homeostasis at every hour of the day. We found that rebound is suppressed in the evening in a *Clk*-dependent manner. We demonstrate that time-dependent rebound is mediated by specific subsets of pacemaker neurons, independently of their effects on locomotor activity. Moreover, homeostatic R5 EB neurons integrate circadian timing and homeostatic drive; we demonstrate that activity dependent and presynaptic gene expression, BRP expression, neuronal output, and wake sensitive calcium levels are all elevated in the morning compared to the evening, providing an underlying mechanism for clock programming of time-of-day dependent homeostasis.

Results

Scheduled sleep deprivation demonstrates suppression of rebound in the evening

To confirm and resolve the timing of clock modulation of sleep rebound, we scheduled sleep deprivation in flies at different times of day and assessed sleep rebound, a protocol we term scheduled sleep deprivation (SSD). We employed an ultradian 7h cycle over 7 days allowing us to observe rebound at each hour of the 24 hour day (24 total deprivations) (Figure 1a,b). SD was administered for 2.5 hours followed by 4.5 hours of rebound such that flies would be allowed ~⅔ of the day to sleep, similar to the ratio of sleep observed in a WT female fly without SD. Given

the potential for stress effects of longer deprivation typically used in flies (6-24h) we opted for a shorter 2.5 h protocol. To test if SSD modulated the circadian phase, SSD flies released into constant dark (DD) following the protocol did not exhibit any detectable change in phase (Figure 1c). There was no significant difference between total sleep in flies kept in SSD and those under baseline conditions (Figure 1d). In addition, sleep rebound does not increase over the course of the 7 day protocol further suggesting that flies are able to fully recover sleep during the 4.5 h rebound period (Figure 1e). Together these results demonstrate that the SSD protocol allows assessment of rebound at different times of day without altering total sleep or circadian phase.

By comparing flies' baseline sleep to their rebound sleep (sleep after deprivation) around the clock, we observed robust rebound in the morning and suppressed rebound in the evening (Figure 2a). Under baseline conditions, flies typically show morning and evening peaks in wakefulness/activity. After sleep deprivation, flies display a robust sleep rebound throughout the 4.5 h rebound period in the morning while evening rebound is suppressed (Figure 2a). To statistically compare morning and evening times of day here and throughout this study, we selected specific time points where the amount of sleep deprived and the baseline sleep during the rebound, two potential confounds, were comparable, allowing a direct comparison of sleep rebound. We also include standardized time points (ZTs 1.5 and 9.5) in the figure supplements for within time point comparisons. As indicated in the heat map, we found sleep rebound in the morning is significantly higher than sleep rebound in the evening when controlling for baseline sleep such that there is a >2x difference in rebound between morning and evening time points (rebound at ZT1.5~133 min and ZT9.5~51 min) (Figure 2b). This was also accompanied by a significant difference in latency following deprivation (Figure 2 figure supplement d). We observed similar results using a streamlined protocol focusing on morning (ZT1.5 and 2.5) and

evening timepoints (ZT8.5, 9.5, 10.5) (Figure 2 figure supplement a). During the course of our experiments, we transitioned to a more streamlined protocol to reduce the length of the protocol and the number of sleep deprivations, minimizing the potential for trends in sleep over the course of the protocol. Video evidence confirms that these morning/evening differences are not due to failure to cross the infrared beam due to increased feeding (Videos 1,2). Lastly, we determined if these effects persist under constant darkness (DD). We observed elevated rebound in the morning (CT2.5) relative to the evening (CT10.5), indicating that these differences are not dependent on light (Figure 2c). Altogether, this data suggests that homeostatic rebound sleep is strongly modulated by the internal clock.

Sleep rebound is dependent on the molecular clock

To determine if morning/evening differences in rebound are due to the circadian clock we performed SSD in arrhythmic Clk^{out} (E. Lee et al., 2014) and short-period per^{s} mutants, which have an advanced evening peak in LD (Hamblencoyle, Wheeler, Rutila, Rosbash, & Hall, 1992; Konopka & Benzer, 1971). In the absence of *Clk*, flies do not display the wild-type morning and evening peaks of wakefulness and exhibit robust rebound at all times, reaching maximal levels of sleep after each SD (Figure 2b). Selected morning/evening time points do not exhibit significant differences in rebound in LD (ZT1.5 and ZT9.5) nor in DD (CT2.5 and CT10.5) (Figure 2e, f). There was also no difference in latency between baseline sleep matched morning and evening time points (ZT1.5 and ZT8.5) after sleep deprivation in Clk^{out} (Figure 2 figure supplement e). Similar to wild-type flies, per^{s} showed elevated rebound in the morning compared to the evening; however, as expected, the trough of rebound sleep in the evening was phase advanced relative to wild-type by about 4 hours (ZT5.5 v. ZT9.5) (Figure 2 figure supplement b,c). Furthermore, per^{s}

flies exhibit an increased sleep latency following deprivation in earlier evening time points (ZT7.5) relative to control (ZT9.5) (Figure 2 figure supplement c). The loss of a morning/evening difference in rebound in arrhythmic *Clk*^{out} and the phase advance of evening rebound suppression in *per*^{s} further support the role of the clock in regulating sleep rebound.

Glutamatergic DN1p circadian pacemaker neurons mediate morning and evening differences in rebound

To address the underlying neuronal basis, we employed a "loss-of-function" approach where we inactivated and/or ablated targeted neuronal populations and assessed the impact on sleep rebound at different times of day. To test the role of clock neurons, we selectively ablated subsets by expressing the pro-apoptotic gene *head involution defective* (*hid*) using the Gal4/UAS system.

Ablation of most of the pacemaker neurons including those underlying morning and evening behavior using *cry39-Gal4* (Klarsfeld et al., 2004; Picot, Cusumano, Klarsfeld, Ueda, & Rouyer, 2007) substantially reduced both morning and evening anticipation in males (Supplemental Table 1) as previously described (Stoleru et al., 2004). Anticipation in females is more difficult to quantify due to more consolidated sleep and wake, i.e., sleep at night reduces morning anticipation, more mid-day wake reduces evening anticipation (Isaac, Li, Leedale, & Shirras, 2010). Consistent with the loss of circadian function, ablation also abolished the difference between baseline sleep matched morning and evening rebound (Figure 3 a, b), displaying high rebound across time points (Figure 3 figure supplement a,b). This effect was also observed using standardized morning and evening (ZT1.5\9.5) time points in which baseline sleep was not matched (Figure 3 figure c). This effect appears to be predominantly due to

197 elevated rebound in the evening (Figure 3 supplement e). We ablated PDF$^+$ using *pdf-Gal4*,
198 which we verified by observing substantially reduced morning anticipation in males validating
199 our reagent (Supplemental table 1). Nonetheless we still observed substantially higher rebound in
200 the morning (ZT1.5) versus the evening (ZT9.5) (Figure 3 c). Moreover the examination of
201 rebound using our full SSD does not indicate a clear change in phase that could explain these
202 results (Figure 3 figure supplement c)Coupling *cry39-Gal4* with *pdf-Gal80* to ablate most clock
203 cells except PDF$^+$ neurons confirms this observation; these flies display high rebound across
204 time points (Figure 3 figure supplement d) and comparably high rebound in baseline sleep
205 matched morning and evening time points similar to *cry39-Gal4* (Figure 3d), highlighting the
206 role of non-PDF clock neurons.
207 Potential synaptic targets of the PDF$^+$ sLNv that are also important for morning behavior
208 are the Glu$^+$ DN1p neurons (Chatterjee et al., 2018; L. Zhang et al., 2010; Y. Zhang, Liu,
209 Bilodeau-Wentworth, Hardin, & Emery, 2010). Targeting of the Glu$^+$ DN1p has relied on drivers
210 that are expressed outside of the DN1p including other sleep regulatory neurons (Chatterjee et
211 al., 2018; Guo et al., 2016). To more definitively test their function, we employed the
212 intersectional split Gal4 system (Dionne, Hibbard, Cavallaro, Kao, & Rubin, 2018) utilizing two
213 promoters, *R18H11* (expressed in DN1p and other neurons) (Guo et al., 2016) and *R51H05* that
214 uses the vesicular glutamate transporter (vGlut) promoter, presumably targeting glutamatergic
215 neurons. This intersection resulted in expression in just 6-7 neurons per hemisphere with little or
216 no expression elsewhere in the brain. Selective labeling of dendritic and axonal arbors using
217 DenMark (Nicolai et al., 2010) and synaptotagmin gfp (Y. Q. Zhang, Rodesch, & Broadie, 2002)
218 , respectively, demonstrated that these neurons show presynaptic projections to both the pars
219 intercerebralis(PI) and more modestly to the lateral posterior neuropil (Figure 4a-c), the latter

consistent with a previous report(Lamaze et al., 2018). We targeted *hid* expression using this split Gal4, we observed a reduction in morning anticipation in males demonstrating the necessity of this defined neuronal group (Supplemental Table 1). However, in females used in our protocols, we did not observe a reduction in morning anticipation, possibly due to the lights-on activity peak masking anticipation (Figure 4 d-f). We also did not observe significant changes in baseline sleep levels (Figure 4g). Despite the lack of a significant change in their baseline sleep/activity profiles, ablation suppressed the difference in morning and evening rebound observed in both Gal4 and hid controls, although there was still a trend towards a morning-evening difference (Figure 4h-j). This effect was also observed using standardized morning and evening (ZT1.5\9.5) time points in which baseline sleep was not matched (Figure 4 figure supplement c,d). There was a significant difference in sleep gain at ZT1.5 between hid control flies and Glu^{+} DN1p ablated flies but did not reach significance with the Gal4 controls (Figure 4i). Overall this indicates that Glu^{+} DN1ps may mediate differences between morning and evening rebound largely independent of their role in regulating baseline sleep/activity.

TuBu and R2/R4m neurons are important for time-dependent modulation of sleep homeostasis

A subset of DN1ps send anterior projections to TuBu interneurons which in turn target the R2/R4m neurons of the EB (Guo et al., 2018; Lamaze et al., 2018)(Figure 4a and 5a). TuBu neurons are a heterogeneous group distinguished by their axonal projections to 3 regions (superior, anterior and inferior) of the Bulb (BU), a neuropil comprised of, among other things, dendritic projections of neurons that form the EB (Lovick, Omoto, Ngo, & Hartenstein, 2017; Omoto et al., 2017). Previous studies have highlighted the role of the superior projecting TuBu

neurons in generating sleep (Guo et al., 2018; Lamaze et al., 2018). To validate and further resolve this circuitry, we mined the Janelia Farm connectome which uses a large-scale reconstruction of the central brain from electron microscopy data (Scheffer et al., 2020). Using this approach, we identified direct synaptic connections from a subset of DN1pB (body IDs: 386834269, 5813071319) to a subset of TuBu neurons (TuBu01), to R4m neurons and eventually to R2 neurons (Figure 5 figure supplement 1a,b). Based on their morphology the Tubu01 neurons are anterior\inferior projecting. Thus, this connectome analysis both validated this circuit but also provided higher resolution for specific subsets that may be involved.

To determine if these neurons are important for sleep homeostasis, we first tested Gal4 drivers previously used to mark these neurons (Guo et al., 2018; Lamaze et al., 2018; Liang et al., 2019; Liu et al., 2016) in combination with *hid*, but found that in many cases (*R52B02*, *R20D01*) they were lethal, likely due to broader anatomic and/or developmental expression. So instead, we used the inward rectifying potassium channel *Kir2.1*(Baines, Uhler, Thompson, Sweeney, & Bate, 2001) to silence these neurons and examined sleep rebound in the morning and evening. Silencing of a previously used driver (*R92H07*) that labels superior projecting TuBu neurons had no effect on rebound (Figure 5- figure supplement 1c,d). We identified another GAL4 driver (*R52B02*) that labels the superior and anterior and/or inferior subgroups previously implicated in sleep regulation (Guo et al., 2018; Jenett et al., 2012; Lamaze et al., 2018). We used this line in combination with *Kir2.1* and found that the difference between morning and evening rebound was lost, similar to what was observed after Glu^{+} DN1p ablation (Figure 5b,c). We knocked down the expression of a metabotropic glutamate receptor (mGluR) in these neurons using RNAi (Guo et al., 2016) and observed phenotypes very similar to silencing them (Figure 5d,e). To determine which neurons are acting downstream of TuBu, we

targeted the R2/R4m neurons using *R20D01*(Lamaze et al., 2018). Silencing these neurons with *Kir2.1* eliminated the difference in rebound between baseline sleep matched morning and evening time points, phenocopying TuBu silencing (Figure 5f). This effect was also observed using standardized ZT1.5/9.5 morning/evening time points in which baseline sleep was not matched (Figure 5- figure supplement 2a-c). Taken together, these results demonstrate a role for the DN1p-Tubu-R2/R4m circuit in regulating time-dependent sleep rebound.

PDF$^-$ sLNv and LNds mediate evening suppression of sleep rebound

To determine the cellular basis of the evening rebound phenotype, we selectively ablated 2-3 LNds and the 5th sLN$_v$ (4 neurons) using the highly specific MB122B split Gal4 line(Guo, Chen, & Rosbash, 2017). This manipulation resulted in high rebound across time points in SSD (Figure 6 figure supplement 1a,b) similar to what was observed in *Clk^{out}* mutants. Furthermore, the difference in sleep gain between baseline sleep matched morning and evening time points was abolished (Figure 6a-c). This effect appears to be due to a large(2-6 fold) increase in rebound in the evening (Figure 6d), with a more modest(~1.5 fold) effect in the morning (Figure 6e).We observed similar results with Kir2.1 (Figure 6 figure supplement 2a,b). Surprisingly we did not observe significant effects on anticipation(Figure 6f-g) (Figure 6- figure supplement 2c,d) or baseline sleep levels by ablation (Figure 6i) or silencing(Figure 6- figure supplement 2e). Differences between these baseline anticipation results and previously observed silencing effects on sleep may be due the use of constitutive versus inducible silencing (Guo et al., 2017). Nonetheless, these results indicate that the effects on rebound are largely independent of baseline anticipation/sleep levels. Thus, just 4 PDF$^-$ LNd/sLNv cells are essential for clock control of rebound with an especially strong suppressive effect in the evening.

PPM3, R5 and dFB neuron synaptic output is required for intact sleep homeostasis

The PPM3 and R5 neurons have been implicated as downstream of the LNd (Figure 7a) (Liang et al., 2019. To test the effects of PPM3 on sleep homeostasis we blocked synaptic transmission by expressing tetanus toxin (TNT) {Sweeney, 1995) using *R92G05-Gal4* (Liang et al., 2019) and a. novel split GAL4 targeting R5 neurons (*R58H05 AD; R48H04 DBD*) (Figure 7b) As LNd calcium oscillations are synchronized with those in the PPM3, we hypothesized that PPM3 silencing may phenocopy LNd ablation, i.e., increasing rebound in the evening. However, while PPM3 silencing did reduce the difference in rebound between baseline sleep matched morning and the evening time points (Figure 7 c,d), this effect appears to be due to dramatically reducing rebound in both the morning and evening (Figure 7 figure supplement 2a,b. Therefore, if homeostatic relevant LNd output is targeting PPM3 neurons, it is inhibiting rather than exciting these neurons. Blocking R5 synaptic output also reduced rebound in both morning and evening (Figure 7- figure supplement 2a, b), consistent with the role of these neurons in mediating rebound from 12 h SD terminating in the morning (Liu et al., 2016). Moreover, no difference between baseline sleep matched morning and evening rebound was evident (Figure 7e,f). R5 neurons promote sleep in response to deprivation by activating the sleep promoting dFB (Liu et al., 2016). Thus, we also blocked synaptic output from the dFB using TNT. Rebound at both morning and evening time points was reduced (Figure 7- figure supplement 2a, b) similar to what was reported for rebound beginning in the morning (Qian et al., 2017). This too resulted in no difference in rebound between baseline sleep matched morning/evening time points as it was for PPM3 and R5 (Figure 7g,h). Although the exact nature of the PPM3 input remains an open

question, these studies highlight a role for a PPM3-R5-dFB pathway in rebound sleep in response to deprivation at all times of day even with shorter deprivation protocols.

R5 ellipsoid body neurons exhibit elevated expression of activity-dependent and presynaptic genes in the morning relative to the evening

To ascertain how the circadian system may impact the R5 homeostat, we examined molecular and physiological changes in R5 as a function of time and sleep need. Interestingly, activation and deprivation studies have focused exclusively on morning rebound. To identify time- and wake-dependent gene expression in an unbiased manner, we selectively labeled R5 neurons (Figure7b, *R58H05 AD; R48H04 DBD > GFP*) and subjected flies to 2.5 h of mechanical SD in either the morning or evening. We then isolated R5 neurons from control or SD flies at ZT1 and ZT9 using fluorescence-activated cell sorting and subjected them to RNA-sequencing.

Based on our behavioral data, we hypothesized that morning SD would induce differential gene expression compared to control flies that did not receive SD while evening SD would not be sufficient to induce changes in gene expression compared to controls. We were surprised to find that neither morning nor evening SD had much of an effect on gene expression in the R5 neurons (Figure 8a,b). In the morning, only two genes were significantly differentially expressed ($q<0.1$, *Hsp70Bb* and *stv*). Likewise, in the evening, only four genes were significantly differentially expressed ($q<0.1$, *CG5522, CG13285, mt:ND5,* and *Hsp70Bb*). In stark contrast, comparisons of morning and evening timepoints with or without sleep deprivation (Morning Control (MC) vs Evening Control (EC), Morning SD (MSD) vs Evening SD (ESD), or MC + MSD vs EC + ESD) produces 46-128 differentially expressed genes ($q<0.1$, Figure 8c,d,e). Notably, this time-of-day dependent regulation does not appear to be driven by core clock genes

in these neurons ((Figure 8- figure supplement) . *Clk* is detected in only 2 out of 12 samples and only at very low levels in those samples with the expression of other clock genes like *per* and *tim* not fluctuating between the two timepoints.

To understand what sorts of molecular programs are undergoing differential regulation between morning and evening, we examined gene ontologies of genes upregulated in the morning. These terms include cellular components like “presynaptic active zone”, “synaptic vesicle”, “terminal bouton”, and “cAMP-dependent protein kinase complex”, as well as molecular functions like “calcium ion binding” and “calcium, potassium::sodium antiporter activity”. The genes identified in these categories suggest a temporally regulated state of activity for the R5 neurons. Indeed, major active zone regulators such as *Syx1A*, *Rim*, *unc-104*, *Srpk79D*, and *nSyb* are all significantly upregulated in the morning (Figure 8e,f). *Syx1A*, *Rim*, and *nSyb* are part of the synaptic vesicle docking and exocytosis machinery and *Rim* also regulates the readily-releasable pool of synaptic vesicles, playing a major role in presynaptic homeostasis (Broadie et al., 1995; Muller, Liu, Sigrist, & Davis, 2012). *unc-104* is involved in trafficking of synaptic vesicles and BRP to the active zone (Y. V. Zhang et al., 2017) and the kinase *Srpk79D* regulates trafficking and deposition of BRP at active zones via phosphorylation of its N-terminus (Johnson, Fetter, & Davis, 2009; Nieratschker et al., 2009). We also observed significant upregulation of genes involved in ionic transport across the plasma membrane, including *para*, a voltage-gated sodium channel (Catterall, 2000; Loughney, Kreber, & Ganetzky, 1989), and *CG5890*, a predicted potassium channel-interacting protein (KChIP) (Figure 8e,g). Mammalian KChIPs have been shown to interact with voltage-gated potassium channels, increasing current density and conductance and slowing inactivation(An et al., 2000). Two sodium:potassium/calcium antiporters, *CG1090* and *Nckx30C*, were also upregulated (Figure

8e,g) . These antiporters function primarily in calcium homeostasis by using extracellular sodium and intracellular potassium gradients to pump intracellular calcium out of the cell when calcium levels are elevated (Haug-Collet et al., 1999). Amongst the most significantly upregulated genes in our dataset, we found six genes that were previously identified as activity-regulated genes in *Drosophila* (ARGs; *sr, Cdc7* (also known as *l(1)G0148*), *CG8910, CG14186, CG17778, hr38*) (Figure 8e,h). These genes are analogous to immediate early genes in mammals and represent half of a group of twelve genes that were induced in three distinct paradigms of neuronal stimulation (X. Chen, Rahman, Guo, & Rosbash, 2016). Finally, we found that several critical components of Creb signaling were enriched in the morning in R5 neurons (Figure 8e,i). *CrebA* was the most significantly upregulated gene in the morning samples, though we also saw significant increases in *meng*, which encodes a kinase that works synergistically with the catalytic subunits of PKA to phosphorylate and stabilize CREBB(P. T. Lee et al., 2018), as well as both regulatory subunits of PKA (*Pka-R1, Pka-R2*) (Figure 8e,i). CREBA and CREBB likely serve different roles, but appear to be involved in activity-dependent processes like dendritogenesis and long term memory (Iyer et al., 2013; Yin, Del Vecchio, Zhou, & Tully, 1995).

Synthesizing these data, it appears that a complex time-dependent program of transcriptional regulation is in play in the morning to upregulate the activity of R5 neurons (Figure 8j). Upregulation of *unc-104, Srpk79D, Syx1a, Rim,* and *nSyb* suggests that R5 neurons are assembling a greater number of mature active zones for neuronal output. Upregulation of *para* and the predicted KChIP *CG5890*, which should increase the voltage-gated conductance of sodium and potassium ions across the membrane, supports the idea that R5 neurons may be primed for greater action potentials in the morning. Upregulation of the two

sodium:potassium/calcium antiporters suggests that intracellular calcium levels are elevated in the morning, again consistent with the idea that these neurons are more active in the morning. Significantly elevated levels of six ARGs also support this conclusion. Finally, there is some suggestion that the elevated activity may result in plasticity in the R5 neurons supported by PKA and CREB signaling.

R5 neurons exhibit time dependent changes in BRP and calcium response to SD

SD/extended wake results in the upregulation of many synaptic proteins (Gilestro, Tononi, & Cirelli, 2009). Most notable is the presynaptic scaffolding protein BRP, important for synaptic release (Matkovic et al., 2013), and is upregulated in the R5 neurons following 12 hrs of SD (Liu et al., 2016). KD of *brp* in R5 neurons decreases rebound response to SD (Huang et al., 2020), suggesting that it is necessary for accumulating and/or communicating homeostatic drive. We hypothesized that differences in the propensity for R5 to induce sleep rebound in the morning/evening may be due to changes in synaptic strength that can be observed by tracking levels of BRP.

To test this idea, we used the synaptic tagging with recombination (STaR) system to selectively express a V5 epitope-tagged BRP in R5 neurons using the FLP/FRT system (Y. Chen et al., 2014) as previously reported (Liu et al., 2016). We examined BRP at ZT1.5 and ZT9.5 with and without SD and found that BRP levels are higher at ZT1.5 than ZT 9.5 (Figure 9a, b). Interestingly, 2.5 h SD had no effect on BRP intensity at either time point (Figure 9b). It is possible that BRP changes in response to 2.5 h of SD are not observable, while a longer 12 h deprivation is required to induce sufficient changes for observation(Liu et al., 2016). We next tested the same two time points in the Clk^{out} mutant background and found no significant

403 difference between ZT1.5 and ZT9.5 (Figure 9b). As reduced BRP expression in the R5 reduces
404 rebound (Huang et al., 2020), it is possible that clock-dependent changes in expression of BRP
405 and associated presynaptic modifications are driving the difference in rebound observed in
406 morning/evening.
407 The calcium concentration in R5 neurons increases following twelve hours of SD,
408 suggesting that extended wakefulness can induce calcium signaling in these neurons. Blocking
409 the induction of calcium greatly reduces rebound, supporting a critical role for calcium signaling
410 in behavioral output (Liu et al., 2016). Furthermore, R5 neurons display morning and evening
411 cell-dependent peaks in calcium activity across the course of the day indicating that calcium is
412 also modulated by the clock network (Liang et al., 2019). It is unclear whether the circadian
413 clock can modulate wake-dependent changes in calcium activity in the R5 neurons.
414 To test this idea, we expressed the calcium reporter GCaMP6s (T. W. Chen et al., 2013)
415 in the R5 and examined calcium in the morning (ZT1.5) and evening (ZT9.5) with and without
416 SD (Figure 9a). Interestingly there was no difference between the non-SD flies at each time point
417 (Figure 9c). One study showed elevated calcium at a later evening timepoint (ZT12; Liu et al.,
418 2016). Our finding of similar calcium levels may be because the morning time point resides on
419 the downswing of the morning-peak of R5 calcium activity while the evening time point resides
420 on the upswing of the evening calcium peak (Liang et al., 2019). Nonetheless, an SD induced
421 increase in calcium was observed in the morning but suppressed in the evening (Figure 9c),
422 suggesting that the R5 sensitivity to sleep deprivation is gated by the clock.
423

Discussion

Here we describe the neural circuit and molecular mechanisms by which discrete populations of the circadian clock network program the R5 sleep homeostat to control the homeostatic response to sleep loss. We developed a novel protocol to administer brief duration SD and robustly measure homeostatic rebound sleep. Using this strategy, we demonstrated that homeostatic rebound is significantly higher in the morning than in the evening. We then identified distinct subsets of the circadian clock network and their downstream neural targets that mediate the enhancement and suppression of morning and evening rebound respectively. Using unbiased transcriptomics, we observed very little gene expression significantly altered in response to our 2.5 h sleep deprivation. On the other hand, we did identify elevated expression of activity-dependent and presynaptic genes in the morning independent of sleep deprivation. Consistent with this finding, we also observe elevated levels of the presynaptic protein BRP that is absent in the absence of *Clk*. These baseline changes are accompanied by an elevated calcium response to sleep deprivation in the morning mirroring the enhanced behavioral rebound in the morning. Taken together, our data support the model of a circadian regulated homeostat that turns the homeostat up late at night to sustain sleep and down late in the day to sustain wake.

Our studies suggest that homeostatic drive in the R5 neurons is stored post-transcriptionally. As part of our studies, we developed a novel protocol using minimal amounts of SD which could be useful for minimizing mechanical stress effects and isolating underlying molecular processes crucial for sleep homeostasis. 6-24 hours of SD in *Drosophila* is commonly used despite the potential stressful or even lethal effects(Fernandez et al., 2014; Shaw, Tononi, Greenspan, & Robinson, 2002; Vaccaro et al., 2020). Here we demonstrate that shorter 2.5 hour deprivations not only induce a robust rebound sleep response (Figure 2), but also the percent of

447 sleep lost recovered at ZT0 is close to 100% versus 14-35% seen in 12 h SD protocols(Blum et
448 al., 2021; Kayser, Yue, & Sehgal, 2014; Nall & Sehgal, 2013; Oh et al., 2014). Using this shorter
449 SD, we now find that many effects observed in R5 neurons with 12 h SD (e.g., increased BRP
450 and upregulation of *nmdar* subunits) are no longer observed with shorter SD, even though the
451 necessity of R5 neurons for rebound is retained after 2.5 h SD (Figure 7e,f). Previously,
452 translating ribosome affinity purification (TRAP) was used to show upregulation of *nmdar*
453 subunits following 12 h SD (Liu et al., 2016).FACS and TRAP are distinct methodologies for
454 targeted collection of RNA for sequencing and can yield unique gene lists (Cedernaes et al.,
455 2019). One possibility is that upregulation of *nmdar* subunits is occurring locally in neuronal
456 processes, which are often lost during FACS, and/or is at the level of translation initiation or
457 elongation. Nonetheless, in agreement with previous work, we observed SD-induced increases in
458 calcium correlated with behavioral rebound in the morning, suggesting that this process is a core
459 feature of the cellular homeostatic response.
460 Using genetically targeted "loss-of-function" manipulations, we have defined small
461 subsets of circadian clock neurons and downstream circuits that are necessary for intact clock
462 modulation of sleep homeostasis. The use of intersectional approaches enabled highly resolved
463 targeting not possible with traditional lesioning experiments in the SCN(Easton et al., 2004).
464 Collectively our studies defined a potential Glu^{+} DN1p-TuBu-R4m circuit important for
465 enhancing morning rebound as well as a discrete group of LNds important for suppressing
466 evening rebound. Importantly, most of these effects on sleep rebound are evident in the absence
467 of substantial changes in baseline activity, despite other studies indicating their necessity for
468 normal circadian behavior. Of note, the proposed roles of the DN1p and LNd clock neurons are
469 sleep (Guo et al., 2016) and wake promotion (Guo et al., 2018) consistent with our findings after

sleep deprivation. We hypothesize that by using chronic silencing methods, baseline effects may not be evident due to compensatory changes but that these effects are only revealed when the system is challenged by sleep deprivation. Similar genetic strategies in mammals (see (Collins et al., 2020)) may be useful in uncovering which SCN neurons are driving circadian regulation of sleep homeostasis given the comparable suppression of sleep rebound in the evening in humans (Dijk & Czeisler, 1994, 1995; Dijk & Duffy, 1999; Lazar et al., 2015). Nonetheless, the finding of sleep homeostasis phenotypes in the absence of significant baseline effects suggests that a major role of these clock neuron subsets may be to manage homeostatic responses.

Our studies suggest that circadian and homeostatic processes do not compete for influence on a downstream neural target but that the circadian clock programs the homeostat itself. Using an unbiased transcriptomic approach, we discovered time-dependent expression of activity dependent and presynaptic genes (Figure 8), consistent with previous data that the R5 neurons exhibit time-dependent activity (Liang et al., 2019; Liu et al., 2016). We observed significant upregulation of several genes involved in synaptic transmission (*Syx1a, Rim, nSyb, unc-104, Srpk79D, para, CG5890*) evincing a permissive active state for R5 neurons in the morning. This is accompanied by elevated levels of the key presynaptic protein BRP in the morning compared to evening. It is notable that elevated BRP in the morning is the opposite of what would be expected based on a sleep-dependent reduction in BRP proposed by the synaptic homeostasis hypothesis (Tononi & Cirelli, 2014), suggesting a sleep-wake independent mechanism. Previous studies have shown that modulation of BRP levels in the R5 are important for its sleep function (Huang et al., 2020), suggesting that changes in BRP levels impact R5 function. We hypothesize that these baseline transcriptomic changes underlie the differential R5 sensitivity to sleep deprivation is evident as calcium increases in the morning and not the

evening. Indeed, trancriptomic and proteomic studies of the mouse forebrain across time and after sleep deprivation are consistent with the model that the circadian clock programs the transcriptome while homeostatic process function post-trranscriptionally (Bruning et al., 2019; Noya et al., 2019), paralleling what we have found for R5. It will be of great interest to understand the circuit and molecular mechanisms by which circadian clocks regulate the R5 neuronal calcium and synaptic properties and whether similar circuit architectures underlie daily mammalian sleep-wake.

Acknowledgements

We would like to thank the Bloomington Stock Center and the Vienna Drosophila Resource Center for reagents. We thank the Flow Cytometry Core and NU seq at Northwestern University for their assistance in cell sorting and sequencing. We are grateful to the members of our neighbors in the Gallio, Bass and Turek labs for their advice. This work was supported by National Institutes of Health (NIH) grant (R01NS106955), Dept. of Army grant (W911NF1610584), Training Grants in Circadian and Sleep Research (HL790919 and HL007909), and postdoctoral NRSA grant (NS110183).

Declaration of interests

The authors declare no competing interest

Methods

Fly husbandry and strains

Flies were maintained on a media of sucrose, yeast, molasses, and agar under 12:12 LD cycles at 25°C. 1-3 day old female flies were separated and maintained on standard cornmeal-yeast medium under 12:12 LD cycles at 25°C for 4 nights before experiments began. *Clk*[out] (56754), per^{s} (80919), *pdf-Gal4* (6899), pBDP (*pBDP-Gal4Uw*)(68384), pBDP split (*p65-AD Uw; Gal4-DBD Uw*) (79603), *R23E10-Gal4* (49032), *R69F08-Gal4* (39499), *R58H05 p59AD* (70750), *R48H04 DBD* (69353) *pdf-Gal80* (80940), *R51H05 p65AD* (70720), *R18H11 DBD* (69017), *R92H07-Gal4* (40633), *R52B02-Gal4* (38814), *R20D01-Gal4* (48889), BRPstar (55751)**,** *UAS-GCaMP6s* (42746), *UAS-TNT* (28838), *UAS-kir2.1* (6596) and *UAS-hid* (65403) were obtained from the Bloomington Drosophila Stock Center. *mGluR*-RNAi (1793) was obtained from Vienna Drosophila Resource Center. *MB122B* and *20xUas-IVS-Syn-GFP* was obtained from Janelia Farm.

Behavioral assays

Following aging and entrainment, 4-7 day old flies were placed in individual 5×65 mm glass capillary tubes containing sucrose-agar food (5% sucrose and 2% agar). These were then loaded into the Drosophila activity monitor (DAM) system (Trikinetics, Waltham, Massachusetts, USA) and placed in either an empty incubator or, in the case of SD experiments, on a multi-tube vortexer (VWR-2500) fitted with a mounting plate (Trikinetics, Waltham, Massachusetts, USA).

For SD experiments 3 nights (with 2 full days) of undisturbed sleep in 12:12 LD cycling at 25°C served as an acclimation period and baseline. Following the baseline period, SD mechanical stimuli was performed as previously described (Nall & Sehgal, 2013). A 2 second

vibration stimulus was applied approximately every 20 seconds with a randomized protocol for a time period of 2.5 hours. In the case of the forced desynchrony protocol this 2.5 hour stimulus was repeated every 7 hours (allowing for a total of 4.5 hours of rest following each stimulus) 24 times until SD occurred at each hour around the clock (Figure 1a). In abridged experiments this 2.5 hour stimulus was applied 5 times: ZT0, ZT8 and ZT23 of day 3, ZT7 of day 4 and ZT6 of day 5. All behavioral experiments consist of pooled data from multiple runs with independent samples.

For sleep analyses DAM data was processed using custom MATLAB based software Sleep MAT(Sisobhan, Rosensweig, Lear, & Allada, 2022). Activity was measured in 1 minute bins and sleep was identified as 5 minutes of inactivity (Hendricks et al., 2000). For SD experiments only flies deprived of >90% of baseline sleep at each SD interval were analyzed (Pfeiffenberger & Allada, 2012). Sleep gain was calculated as the difference between sleep during rebound and sleep during the equivalent 4.5 hours at baseline. Activity actograms were plotted with Counting Macro as previously described (Pfeiffenberger, Lear, Keegan, & Allada, 2010a, 2010b).

Immunostaining

Following aging and entrainment, 4-7 day old flies were placed in individual tubes containing sucrose-agar food (5% sucrose and 2% agar) for 3 nights. Brains were dissected in PBS (137mM NaCl, 2.7mM KCl, 10mM Na2HPO4 and 1.8mM KH2PO4) and fixed in 3.7% formalin solution (diluted from 37% formalin solution, Sigma-Aldrich) for 30 minutes at 4°C. Brains were washed with 0.3% PBSTx (PBS with 0.3% Triton-X) 5 times (with 15 minute shaking steps at 4°C) before primary antibody incubation. Primary antibodies were diluted in 0.3% PBSTx with 5%

normal goat serum and incubation was done at 4°C overnight. Brains were washed for 5 times with 0.3% PBSTx. Secondary antibodies were diluted in 0.3% PBSTx with 5% normal goat serum and brains were incubated at 4°C overnight. Primary antibody used was mouse anti-V5 (1:800 Invitrogen), Secondary antibody used was Alexa 594 anti-mouse (1:800, Invitrogen).

Images were taken using Nikon C2 confocal at 63x magnification and acquired at 1,024 x 1,024 pixels. Analysis of BRP intensity was performed using Fiji/Imagej similarly to previously reported methods (Liu et al., 2016). First max intensity projections were created from confocal stacks of R5 ring projections. The mean intensity of the R5 ring was analyzed by subtracting the average intensity of an adjacent region (background) from the average intensity of the R5 projections. Imaging data presented are derived from a single experiment due to inability to pool data from multiple experiments because of changes in laser condition and staining. All experiments were replicated a minimum of 3 times to confirm results.

Intracellular $Ca2^+$ measurements

Following aging and entrainment, 4-7 day old *R69F08-Gal4 > UAS-GCaMP6s*, UAS-CD4-tdTomato flies were placed in individual tubes containing sucrose-agar food (5% sucrose and 2% agar) for 3 nights. Flies were dissected day 4 and imaged in ice-cold control *Drosophila* physiological saline solution (in mM: 101 NaCl, 1 $CaCl_2$, 4 $MgCl_2$, 3 KCl, 5 glucose, 1.25 NaH_2PO_4, and 20.7 $NaHCO_3$, pH 7.2, 250 mOsm) (Flourakis et al., 2015). Brains were held ventral side down by a harp slice grid with silica fibers from ALA scientific. GCaMP and TdTomato signal in the R5 ring neuropil was measured immediately (within 5 min) after dissection at ZT1.5 and ZT9.5. Imaging experiments were performed on an Ultima two-photon laser scanning microscope (Bruker, former Prairie Technologies, Middleton, WI). Images were

acquired with an upright Zeiss Axiovert microscope with a 40×0.9 numerical aperture water immersion objective at 512 pixels × 512 pixels resolution. Single optical R5 section was selected and recorded as previously described (Liu et al., 2016). In brief a single optical section was selected based on visual assessment of maximum area of tdtomato signal. The GCaMP signal was recorded at ~1 fps for 60 seconds. The average projection of the frames was used to calculate the GCaMP and TdTomato signal.

Connectome analysis

We accessed the NeuPrint API via R using a Natverse-based software package, *neuprintr*, along with two other open-source data visualization tools, *hemibrainr* and *ggplot2*(Bates, Manton, et al., 2020; Bates, Schlegel, et al., 2020) . R scripts provided by the Natverse creators were modified to generate connectivity graphs (node networks) and neuron skeletonizations (visualizations of neuronal morphology). Our modified scripts can be found at https://rpubs.com/eogunlana0827/modified-code-for-analysis. Most of the neurons used in this study were identified based on their annotation in Neuprint. Cry-positive LNds were identified in the total LNd based on morphology according to the images in Schubert et al (Schubert, Hagedorn, Yoshii, Helfrich-Forster, & Rieger, 2018).

To generate node networks for sleep pathways, the body IDs of the pre- and post-synaptic targets were determined by querying the neuron types and storing the retrieved data into two data frames (A and B, respectively). Once A and B were determined, the shortest paths between the two types were then calculated. The code accounts for any duplicates that may arise when running *neuprintr*'s "shortest paths" function. This information is stored in another data frame that represents each pre- and post-synaptic neuron instance in the pathway, along with their

611 names/types and the number of synapses between each neuron. Before establishing the network
612 environment in which the data are plotted, the newly created data frame was modified so that
613 only the pre- and post-synaptic neuron types and synaptic weights were included, thereby
614 removing any body ID information. We then utilized the *network* and *ggnetwork* packages (both
615 under the *ggplot2* package framework) to create the network environment. Colors were assigned
616 to each neuron type using a list of variables provided in the pre-made R scripts. Finally, the
617 connectivity graphs were plotted using *ggplot2* and exported to PDFs.
618 The *hemibrainr* package was used to generate visualizations of neuronal morphology
619 from the EM data underlying Neuprint *(Bates, Manton, et al., 2020)*. For each neuron type in the
620 sleep pathways, we collected the neuron mesh data from their NeuPrint body IDs using a
621 hemibrainr function and then stored them in a variable. Then, we randomly sampled a color to
622 assign to each neuron type using a built-in R function. The neuron mesh was then plotted in a 3D
623 environment, and then oriented so that the anterior side of the brain was facing the viewer.
624
625 **Fluorescence Activated Cell Sorting and RNA-seq**
626 FACS/RNA-seq was performed as previously reported (Xu, Kula-Eversole, Iwanaszko, Lim, &
627 Allada, 2019). Briefly, flies were housed in DAM system behavior boards in either control or
628 sleep deprivation conditions. Immediately following SD, the boards were recovered from the
629 incubators and transferred to CO_2 pads. Brains were dissected in ice-cold modified dissecting
630 saline (9.9 mM HEPES-KOH buffer, 137 mM NaCl, 5.4 mM KCl, 0.17 mM NaH_2PO_4, 0.22 mM
631 KH_2PO_4, 3.3 mM glucose, 43.8 mM sucrose, pH 7.4) with 0.1 μM tetrodotoxin (TTX), 50 μM
632 D(–)-2-amino-5-phosphonopentanoic acid (AP-5), and 20 μM 6,7-dinitroquinoxaline-2,3-dione
633 (DNQX) to block neuronal activity. Following dissection, brains were transferred to SM^{Active}

634 medium (4.18 mM KH_2PO_4, 1.05 mM $CaCl_2$, 0.7 mM $MgSO_4 \cdot 7H_2O$, 116 mM NaCl, 8mM
635 $NaHCO_3$, 2 mg/ml glucose, 2 mg/ml trehalose, 0.35 mg/ml α-ketoglutaric acid, 0.06 mg/ml
636 fumaric acid, 0.6 mg/ml malic acid, 0.06 mg/ml succinic acid, 2 mg/ml yeast extract with 20%
637 non-heat-inactivated FBS, 2 mg/ml insulin and 5mM pH6.8 Bis-Tris) with 0.1 μM TTX, 50 μM
638 AP-5, and 20 μM DNQX on ice while the rest of the brains were dissected. 40-45 brains per time
639 point were pooled as a single sample and every condition and time point was run in triplicate for
640 a total of twelve samples. Following dissection, the brains were pelleted by centrifugation (2000
641 rpm, 1 min) and washed twice with 500 uL of chilled dissecting saline (containing TTX, AP-5,
642 and DNQX). Dissecting saline was removed and the brains were incubated at room temperature
643 in 100 μL of papain (50 unit/mL, heat activated for 10 min at 37ºC) for 30 minutes. Following
644 digestion, the papain was inactivated with 500 μL of chilled SM^{Active} medium and then washed
645 twice with chilled medium on ice. The brains were triturated by pipetting with a flame-rounded
646 1,000 μL pipette tip (30 times with a medium opening, 30 times with a small opening). The
647 sample was filtered using a 100 μm nylon filter (Sefar Nitex 03-100/32) then transferred to the
648 Northwestern FACS core on ice. GFP-positive cells were sorted on an Aria II FACS Cell Sorter
649 into an extraction buffer from the Arcturus PicoPure Kit. We collected 300-550 cells per sample.
650 Following sorting, the cells were lysed in extraction buffer by incubating at 42ºC for 30 min.
651 After lysing, the cells were stored in a -80ºC freezer until libraries could be made. 3 biological
652 replicates for each treatment are included.
653 Total RNA was extracted from collected cells using the PicoPure Kit with on-column
654 DNAse I digestion according to manufacturer instructions. Following extraction, the RNA was
655 immediately concentrated down to 1 μL using a Speed-Vac. First strand cDNA was prepared
656 using a T7-oligo-dT primer and SuperScript III following manufacturer instructions. Second

strand synthesis was performed with DNA Polymerase (18010025), Second Strand Buffer (Cat#10812014), 10 mM dNTP (18427088), DNA Ligase (18052019), and RNaseH (18021071). The cDNA was used as a template for one round of *in vitro* transcription (IVT) using T7 RNA polymerase and the Ambion MegaScript kit according to manufacturer instructions. IVT was carried out at 37.5°C for 4 hours. Following IVT, the new RNA was purified using a Qiagen RNEasy kit and then used to generate libraries for RNA-seq using an Illumina TruSeq Stranded Kit. Libraries were checked for appropriate size distribution and purity by Bioanalyzer, then sent to Novogene for sequencing. We generated 30 million reads per sample.

Reads were pseudo aligned and quantified using Kallisto (v0.46.1) (Bray, Pimentel, Melsted, & Pachter, 2016) against a prebuilt index file constructed from Ensembl reference transcriptomes (v96). Kallisto was used to process paired end reads with 10 bootstraps. Differential expression analysis of the resulting abundance estimate data was then performed with Sleuth (v0.30.0)(Pimentel, Bray, Puente, Melsted, & Pachter, 2017). Gene-level abundance estimates were computed by summing transcripts per million (TPM) estimates for transcripts for each gene. To measure the effect of a particular condition against another condition for a variable, sleuth uses a Wald test which generates *p* values as well as *q* values (an adjusted *p* value using the Benjamini-Hochberg procedure).

Statistics

Statistical analyses and figures were produced with Excel, Matlab and Prism. Statistical tests used, exact values of N, definitions of center, methods of multiple test correction, dispersion and precision measures and p-values are included in figure legends. Paired student T-tests were used to compare 2 groups/time points. Repeated one and two factor ANOVA analyses were used to

compare multiple time points/groups with Tukey's post hoc test. Additional details regarding tests and significance values are provided in the figure legends.

Figure legends

Figure 1 T7 Drosophila forced desynchrony protocol can be used to illustrate time dependent rebound

(A) Average WT sleep (N=32) over the final 8 days of SSD protocol with the time at which rebound begins (ZT) noted below each rebound period. (B) Profiles of sleep metrics used to compare rebound at different times of day (example is rebound occurring at ZT4.5). Sleep lost is determined by the difference between baseline sleep and sleep during the SD. Sleep gain is determined by the difference between rebound and baseline sleep. (C) Average activity of WT flies over 24 hours of flies released into the dark following SSD stimulation (N=19) or control (N=19) that received no stimulation. WT Flies released into DD1 following SSD display a profile of activity similar to control flies. Shaded bands indicate SEM.(D) Average sleep during baseline and the average sleep per day during the 7 day SD-rebound period (individual flies shown circles). There is no significant difference between average baseline sleep and average sleep per day over the course of the SSD ($P>0.08$, paired t-test). (E) Average WT (N=32) sleep gain across the course of the experiment with rebound time (ZT) depicted on the x axis. Regression of WT sleep gain over the course of the experiment displays no significant trend ($P>0.95$ linear regression). Data are means +/- SEM.

Figure 1—source data 1

T7 Drosophila forced desynchrony protocol can be used to illustrate time dependent rebound

Figure 0 Sleep rebound is dependent on the molecular clock

(A,D) Rebound sleep heatmaps (above) illustrate average sleep as a function of time of day when rebound occurred (ZT) and minutes after SSD episode. Missing time points are filled using matlab linear interpolation function. Baseline sleep heatmaps (below) illustrate average sleep during 30 min bins. (A) WT (N=32) baseline displays low sleep following lights on and preceding lights off. Immediately following SD flies show high sleep except in the hours preceding lights off. Flies tend to sleep less as rebound time proceeds. (B,E) Comparison of sleep lost, baseline sleep, and sleep gain following deprivation at morning and evening timepoints. (B) Sleep gain is greater for WT (N=32) rebound at ZT1.5 compared to ZT9.5 (P<.00001, paired t-test). (C,F) Two sleep measures in control flies (control during SD and control during rebound), along with sleep during rebound in SD with rebound at 2.5 and 10.5. (C) Rebound sleep is greater following deprivation at CT2.5 compared to CT10.5 (P<.00001, paired t-test) in WT flies (N= 49). (D) Clk^{out} (N=40) baseline sleep (below) is nearly constant except for low sleep immediately following lights on. SD uniformly increases sleep and flies tend to sleep less as rebound time proceeds. (E) No difference between sleep gain at the two time points is observed in Clk^{out} (N=40) (P>0.37, paired t-test). (F) No difference in rebound sleep is observed in Clk^{out} (N= 23) (P>0.75, paired t-test). Data are means +/- SEM

Figure 2—source data 1

Sleep rebound is dependent on the molecular clock

Figure 3 PDF^{+} neurons do not mediate morning/evening differences in rebound

(A,B,C,D) Comparison of sleep lost, baseline sleep, and sleep gain following deprivation at morning and evening timepoints in clock neuron-ablated flies. Morning times are matched with evening time points with similar baselines. (A) Control flies with no ablated neurons (+ > hid) (N=27) exhibit greater rebound in the morning compared to matched evening time point ($P<0.0001$, paired t-test). (B) Flies with most clock neurons ablated (cry39 > hid) (N=19) exhibit no difference in sleep gain between matched morning/evening time points ($P>0.70$, paired t-test). (C) Files with PDF^+ neurons ablated (pdf > hid) (N=35) exhibit greater rebound in the morning compared to a matched evening time point ($P<0.01$, paired t-test). (D) Flies with most clock neurons ablated except PDF^+ neurons (cry39; pdf-Gal80 > hid) (N=22) exhibit no significant difference in sleep gain between matched morning/evening time points ($P>0.97$, paired t-test). Data are means +/- SEM.

Figure 3—source data 1

PDF^+ neurons do not mediate morning/evening differences in rebound

Figure 4 Glutamatergic DN1ps are necessary for morning and evening differences in rebound

A-C) 20x images of split Gal4 line that labeling presynaptic (A), postynaptic (B) and overlay (C) of Glu^+ DN1ps (R51H05 AD; R18H11 DBD > SYT-GFP; DenMark) co-stained for BRP (blue). (D-F) Averaged activity eductions for female flies during the first 2 days of 12:12 LD. The light-phase is indicated by white bars while the dark-phase is indicated by black bars. Morning and evening anticipation indices are represented in blue and red respectively. (G) Average sleep during the baseline day for Glu^+ DN1ps ablated (R51H05 AD; R18H11 DBD > hid) (N=30)

(green), Gal4 control (R51H05 AD; R18H11 DBD> +) (N=36) and hid control (pBDP split > hid) (N=26) (purple). Sleep per 24 hours is indicated in the bottom right. (H-J) Comparison of sleep lost, baseline sleep, and sleep gain following deprivation at morning and evening timepoints in Glu^{+} DN1p ablated flies. Morning times are matched with evening time points with similar baselines. (H) hid control flies with no ablated neurons (pBDP split > hid) (N=26) exhibit greater rebound in the morning compared to matched evening time point ($P<0.0001$, paired t-test). (I) Gal4 control flies with no ablated neurons (R51H05 AD; R18H11 DBD> +) (N=19) exhibit greater rebound in the morning compared to matched evening time point ($P<0.01$, paired t-test) (J) Flies with Glu^{+} DN1ps ablated (R51H05 AD; R18H11 DBD > hid) (N=21) do not exhibit a significant difference in sleep gain between matched morning/evening time points ($P>0.09$, paired t-test). (K) Comparison of sleep gain at ZT1.5 between flies with Flies with Glu^{+} DN1ps ablated (R51H05 AD; R18H11 DBD > hid) (N=21) and their controls (pBDP split > hid) (N=26) and (R51H05 AD; R18H11 DBD> +) (N=19). R51H05 AD; R18H11 DBD > hid flies exhibit significantly less rebound at ZT1.5 compared to hid control ($P<0.05$, ANOVA) and a non-significant decrease compared to Gal4 control ($P>0.05$, ANOVA). Data are means +/- SEM.

Figure 4—source data 1

Glutamatergic DN1ps are necessary for morning and evening differences in rebound

Figure 5 TuBu intermediates convey enhanced morning glutamatergic signal to R2/R4m ellipsoid body neurons

(A) Cartoon illustrating proposed link between Glu^{+} DN1ps and R2/R4m with Tubu intermediates. (B-F) Comparison of sleep lost, baseline sleep, and sleep gain following

deprivation at morning and evening timepoints while modulating neurons linking DN1ps to the EB. Morning times are matched with evening time points with similar baselines. (B) Enhancerless-Gal4 control flies (pBDP > Kir) (N=21) exhibit greater rebound in the morning compared to a matched evening time point ($P<0.01$, paired t-test). (C) Flies with TuBu neurons silenced (R52B02 > Kir) (N=21) do not exhibit a difference in rebound between matched morning/evening time points($P> 0.38$, paired t-test). (D) Enhancerless-Gal4 driver paired with UAS-GluR-RNAi (pBDP > GluR RNAi) control (N=32) exhibit greater rebound in the morning compared to matched evening time point ($P<0.00001$, paired t-test). (E) Flies with KD of GluR in TuBu neurons (R52B02 > GluR RNAi) do not exhibit a significant difference between matched morning/evening time points ($P>0.28$, paired t-test). (F) Flies with R2/R4m neurons silenced (R20D01 > Kir) (N=32) do not exhibit a significant difference in rebound between matched morning/evening time points($P>0.26$, paired t-test). Data are means +/- SEM.

Figure 5—source data 1

TuBu intermediates convey enhanced morning glutamatergic signal to R2/R4m ellipsoid body neurons

Figure 6 LNds and the PDF- sLNv suppress evening rebound

(A-C) Comparison of sleep lost, baseline sleep, and sleep gain following deprivation at morning and evening timepoints in clock neuron-ablated flies. Morning times are matched with evening time points with similar baselines. (A) hid control flies with no ablated neurons (pBDP split > hid) (N=26) exhibit greater rebound in the morning compared to matched evening time point ($P<0.0001$, paired t-test). (B) Gal4 control flies with no ablated neurons (MB122B> +) (N=29)

796 exhibit greater rebound in the morning compared to matched evening time point (P<0.01, paired
797 t-test) (C) Flies with 2-3 LNds and the PDF- sLNv ablated (MB122B > hid) (N=30) do not
798 exhibit a significant difference in sleep gain between matched morning/evening time points
799 (P>0.50, paired t-test). (D-F) Averaged activity eductions for female flies during the first 2 days
800 of 12:12 LD. Light phase is indicated by white bars while the dark phase is indicated by black
801 bars. Morning and evening anticipation indices are represented in blue and red respectively. (G)
802 Average sleep during the baseline day for LNds and the PDF- sLNv ablated (MB122B > hid)
803 (N=30) (green), Gal4 control (MB122B > +) (N=29) (blue), and hid control (pBDP split > hid)
804 (N=26) (purple). (H, I) Comparison of sleep gain at ZT1.5 (H) and ZT9.5 (I) between flies with
805 2-3 LNds and the PDF- sLNv ablated (MB122B > hid) (N=29) and their controls (pBDP split >
806 hid) (N=26)(MB122B> +) (N=29). MB122B > hid flies exhibit greater rebound at morning (H)
807 (P<0.05, ANOVA) and evening (I) (P<0.001, ANOVA). Data are means +/- SEM
808
809 **Figure 6—source data 1**
810 LNds and the PDF- sLNv suppress evening rebound
811
812 **Figure 7 PPM3 convey enhancing homeostatic signal to R5 ellipsoid body neurons**
813 (A) Cartoon illustrating link between LNds and 5th sLNv and dFB via with PPM3 and R5
814 intermediates. (B) GFP Expression pattern of split Gal4 line that labels Glu^{+} DN1ps (R58H05
815 AD; R48H04 DBD > GFP) at 20x. (C-H) Comparison of sleep lost, baseline sleep, and sleep
816 gain following deprivation at morning and evening timepoints modulating neurons linking LNd
817 activity to the EB. Morning times are matched with evening time points with similar baselines.
818 (C) Flies expressing an inactive form of tetanus toxin in PPM3 neurons (R92G05 >

TNTi)(N=45) exhibit greater rebound in the morning than at a matched evening time point ($P<0.0001$, paired t-test). (D) Silencing PPM3 neurons with an active form of tetanus toxin (R92G05 > TNTa)(N=27) resulted in no significant difference between matched morning/evening time points ($P>0.10$, paired t-test). (E) Flies expressing an inactive form of tetanus toxin in R5 neurons (R58H05 AD; R48H04 DBD > TNTi) (N=21) exhibit greater rebound in the morning than at a matched evening time point ($P<0.01$, paired t-test). (F) Silencing R5 neurons with tetanus toxin (R58H05 AD; R48H04 DBD > TNTa) (N=16) resulted in no significant difference in sleep gain for matched morning and evening time points ($P>0.70$, paired t-test). (G) Flies expressing an inactive form of tetanus toxin in the dFB (R23E10 > TNTi) (N=30) exhibit greater rebound in the morning than at a matched evening time point ($P<0.0001$, paired t-test). (H) Silencing dFB neurons with tetanus toxin (R23E10 > TNTa) (N=12) resulted in no significant difference between morning and evening time points ($P>0.45$, paired t-test).

Figure 7—source data 1

PPM3 convey enhancing homeostatic signal to R5 ellipsoid body neurons

Figure 8 RNA sequencing of FAC-sorted R5 neurons suggests elevated activity in the morning

(A) Volcano plot (fold change versus qval) of Morning SD (MSD) vs Morning Control (MC) gene expression. Significantly differentially expressed genes shown in orange. (B) Volcano plot of Evening SD (ESD) vs Evening Control (MC) gene expression. Significantly differentially expressed genes shown in orange. (C) Volcano plot of MC vs EC gene expression. 51 significantly differentially expressed genes (DEG) were identified and are shown in orange. (D) Volcano plot of MSD vs ESD gene expression. 46 significantly differentially expressed genes

(DEG) were identified and are shown in orange. (E) Volcano plot of MC+MSD vs EC+ESD gene expression. Differentially expressed genes are shown in green with a few genes highlighted in orange and labeled. (F-I) Scatter plots for several differentially expressed genes. Transcripts *Per* Kilobase Million (TPM) is shown for each sample. All morning samples are grouped, and all evening samples are grouped. Graphs are grouped by similar functions: (F) active zone components/regulators, (G) membrane-associated ionic regulators, (H) activity-regulated genes, (I) PKA/CREB signaling. (J) Schematic of select morning upregulated genes. Upregulated genes are shown in color while other interacting components are depicted in gray. PARA and CG5890 are both involved in the generation and propagation of action potentials. Multiple active zone components/regulators (NSYB, SYX1A, RIM, SRPK79D, UNC-104) interact with BRP and voltage-gated calcium channels (VGCCs) to support neuronal output and intracellular calcium influx. Elevated levels of intracellular calcium are regulated by the antiporters NCKX30C and CG1090. Second messenger cAMP interacts with regulatory subunits of PKA (R1/R2) and releases the catalytic subunits (C1/C2) to phosphorylate CREBB and MENG, stabilizing CREBB. CREBA acts as a transcriptional activator independent of PKA activity.

Figure 8—source data 1

RNA sequencing of FAC-sorted R5 neurons suggests elevated activity in the morning

Figure 9: R5 neurons exhibit time dependent changes in BRP and calcium response to SD

(A) Schematic illustrating deprivation and dissection timing for morning (M) and evening (E) with (lower) and without (upper) SD. (B) Fluorescence of BRP-STaR in R5 projections as a function of time of day and SD in WT (left)and Clk^{out} mutant (right) backgrounds. Intensity of

BRP staining is decreased at ZT9.5 compared to ZT1.5 in both control (N= 11, 11)(P< 0.001, independent t-test) and SD (N= 11, 11) (P<0.01, independent t-test) groups. Intensity of BRP staining is not affected by SD in the morning (N=11,11) (P> 0.90, independent t-test) or evening (N=11,11) (P>0.58, independent t-test). Intensity of BRP staining in Clk^{out} mutants is not significantly different at ZT1.5 (N=8) compared to ZT9.5 (N=10) (P>0.36, independent t-test).(D) GCaMP expression in R5 projections (R69F08 > GCamP6s) at ZT1.5 and ZT9.5 with and without SD. GCaMP fluorescence was normalized to the tdTomato fluorescence signal intensity. There is no difference in normalized GCaMP6s signaling between baseline morning (N=10) and evening (N=10) time points. SD in the morning (N=10) increases GCaMP6s intensity (P< 0.05, independent t-test) but not in the evening (N=10) (P>0.87 independent t-test), independent t-test). Data are means +/- SEM.

Figure 9—source data 1

R5 neurons exhibit time dependent changes in BRP and calcium response to SD

Supplementary figure legends

Figure 2-figure supplement 1 Total sleep and sleep latency vary as a function of time and SD

(A) Comparison of sleep lost, baseline sleep, and sleep gain at morning (ZT1.5) and evening (ZT9.5) time points using abridged protocol with WT flies. Sleep gain is greater for WT (N=18) at ZT1.5 compared to ZT9.5 (P<.001, paired t-test). (B) Rebound sleep heatmap (above) illustrates average sleep as a function of time of day when rebound occurred (ZT) and minutes

after SSD episode. Missing time points are filled using matlab linear interpolation function. Baseline sleep heatmaps (below) illustrate average sleep during 30 min bins. pers (N=45) baseline sleep displays low sleep following lights on and preceding lights off. Immediately following SD flies show increased sleep except in the hours preceding lights off. Flies tend to sleep less as rebound time proceeds. (C) FD sleep during two baseline time periods (sleep lost and baseline sleep) and sleep gain for rebound occurring at ZT1.5 and ZT5.5. Sleep gain is greater for pers (N=45) rebound at ZT1.5 compared to ZT5.5 (P<.01, paired t-test). (D-F) Morning and evening sleep latency at baseline and following deprivation for WT and circadian mutant flies. Morning times are matched with evening time points with similar baseline latency. (D) Following SD, WT (N=32) sleep latency is greater in the evening compared to matched morning time point (P<.05, paired t-test). (E) No difference in sleep latency following SD between matched morning/evening time points in Clk^{out} (N=40) (P>0.50, paired t-test). (F) Following SD, pers (N=45) sleep latency is greater in the evening compared to matched morning time point (P<.0001, paired t-test). Data are means +/- SEM.

Figure 2—figure supplement 1—source data 1

Total sleep and sleep latency vary as a function of time and SD

Figure 3-figure supplement 1 Non PDF neurons drive morning/evening differences in rebound(A,B,D,E) Rebound sleep heatmaps (above) illustrate average sleep as a function of time of day when rebound occurred (ZT) and minutes after SSD episode. Missing time points are filled using matlab linear interpolation function. Baseline sleep heatmaps (below) illustrate average sleep during 30 min bins. (A) Control flies with no ablated neurons (+ > hid) (N=27) displays low baseline sleep following lights on and preceding lights off. Immediately following

SD flies show high sleep except in the hours preceding lights off. Flies tend to sleep less as rebound time proceeds. (B) Flies with most clock neurons ablated (cry39 > hid) (N=19) displays low baseline sleep during the day and high sleep at night (below). SD uniformly increases sleep and flies tend to sleep less as rebound time proceeds and following lights on (C) Comparison of sleep lost, baseline sleep, and sleep gain following deprivation at morning and evening timepoints in clock neuron-ablated flies. Morning times are matched with evening time points with similar baselines. Flies with most clock neurons ablated (cry39 > hid) (N=19) do not exhibit a significant difference in sleep gain between the morning and evening time points ($P>0.01$, paired t-test) however exhibit greater sleep lost in the evening ($P<0.05$, paired t-test). (D) Files with PDF^+ neurons ablated (pdf > hid) (N=35) displays low baseline sleep following lights on and preceding lights off. Immediately following SD flies show high sleep except in the hours preceding lights off. (E) Flies with most clock neurons ablated except PDF^+ neurons (cry39; pdf-Gal80 > hid) (N=22) display low baseline sleep during the day and high sleep at night (below). SD uniformly increases sleep and flies tend to sleep less as rebound time proceeds and following lights on. (F) Comparison of sleep gain at ZT9.5 between control flies and flies with most clock neurons ablated. clock neuron ablated flies exhibit significantly greater rebound at ZT9.5 compared to controls ($P< 0.0001$, unpaired t-test).

Figure 3—figure supplement 1—source data 1

Non PDF neurons drive morning/evening differences in rebound

Figure 4-figure supplement 1 Standardized time points show similar effects to points with matched baseline sleep

(A-B) Rebound sleep heatmaps (above) illustrate average sleep as a function of time of day when rebound occurred (ZT) and minutes after SSD episode. Missing time points are filled using matlab linear interpolation function. Baseline sleep heatmaps (below) illustrate average sleep during 30 min bins. (A) Gal4 controls with no ablated neurons (R51H05 AD; R18H11 DBD> +) (N=19) display low baseline sleep following lights on and preceding lights off. Immediately following SD flies show high sleep except in the hours preceding lights off. Flies tend to sleep less as rebound time proceeds. (B) Glu^{+} DN1ps ablated (R51H05 AD; R18H11 DBD > hid) (N=14) flies display low baseline sleep following lights on and preceding lights off. Immediately following SD flies show high sleep except in the afternoon and hours preceding lights off. Flies tend to sleep less as rebound time proceeds. (C,D) Comparison of sleep lost, baseline sleep, and sleep gain following deprivation at morning and evening timepoints in clock neuron-ablated flies. Morning times are matched with evening time points with similar baselines. (C) Gal4 control flies with no ablated neurons (R51H05 AD; R18H11 DBD> +) (N=19) exhibit greater rebound in the morning compared to the evening time point ($P<0.01$, paired t-test) however exhibit greater sleep lost in the evening ($P<0.05$). (D) Flies with Glu^{+} DN1ps ablated (R51H05 AD; R18H11 DBD > hid) (N=14) do not exhibit a significant difference in sleep gain between the morning and evening time points ($P>0.05$, paired t-test) however exhibit greater sleep lost in the evening ($P<0.05$, paired t-test). Data are means +/- SEM.

Figure 4—figure supplement 1—source data 1

Standardized time points show similar effects to points with matched baseline sleep

Figure 5-figure supplement 1 Connectome analysis demonstrates link between anterior projecting DN1ps and R2/R4m ellipsoid body ring neurons.

(A) Node network diagram of pathway from anterior projecting DN1ps to R2/R4m via Tubu intermediates. Arrows indicate directionality of projections and numbers represent average synaptic connections between groups of neurons. (B) Dorsal view of neuronal morphology of pathway from anterior projecting DN1ps to R2/R4m via Tubu intermediates according to Neuprint EM reconstruction. Each cell subtype is color coded to match the model in A. (C-D) Comparison of sleep lost, baseline sleep, and sleep gain following deprivation at morning and evening timepoints while modulating TuBu neurons. Morning times are matched with evening time points with similar baselines. (C) Enhancerless-Gal4 control flies (pBDP > Kir) (N=21) exhibit greater rebound in the morning compared to a matched evening time point ($P<0.01$, paired t-test). (D) Flies with TuBu neurons silenced (R92H07 > Kir) (N=21) exhibit greater rebound in the morning compared to a matched evening time point ($P<0.0001$, paired t-test).

Figure 5—figure supplement 1—source data 1

Connectome analysis demonstrates link between anterior projecting DN1ps and R2/R4m ellipsoid body ring neurons

Figure 5-figure supplement 2 Standardized time points show similar effects to points with matched baseline sleep

(A-C) Comparison of sleep lost, baseline sleep, and sleep gain following deprivation at morning and evening timepoints in clock neuron-ablated flies. Morning times are matched with evening

time points with similar baselines. (A) Enhancerless-Gal4 control flies (pBDP > Kir) (N=21) exhibit greater sleep lost for rebound occurring at ZT9.5 ($P<0.01$, paired t-test) however retain significantly more rebound at ZT 1.5 compared to ZT 9.5 ($P<0.05$, paired t-test).(B) Flies with TuBu neurons silenced (R52B02 > Kir) (N=21) exhibit significantly greater baseline sleep during the rebound period at ZT9.5 ($P<0.0001$), however do not exhibit a difference in sleep gain between ZT 1.5 and ZT9.5 ($P>0.32$, paired t-test).(C) Flies with KD of GluR in TuBu neurons (R52B02 > GluR RNAi) significantly greater sleep lost at ZT 9.5 ($P<0.00001$, paired t-test), and exhibit no significant difference in sleep gain between ZT 1.5 and ZT9.5 ($P>0.66$, paired t-test). Data are means +/- SEM.

Figure 5—figure supplement 2—source data 1

Standardized time points show similar effects to points with matched baseline sleep

Figure 6-figure supplement 1 Full SSD demonstrates loss of evening suppression of rebound in LNd ablated flies

(A-B) Rebound sleep heatmaps (above) illustrate average sleep as a function of time of day when rebound occurred (ZT) and minutes after SSD episode. Missing time points are filled using matlab linear interpolation function. Baseline sleep heatmaps (below) illustrate average sleep during 30 min bins. (A) Gal4 controls with no ablated neurons (MB122B> +) (N=29) display low baseline sleep following lights on and preceding lights off. Immediately following SD flies show high sleep except in the hours preceding lights off. Flies tend to sleep less as rebound time proceeds. (B) Flies with 2-3 LNds and the PDF^- sLNv ablated (MB122B > hid) (N=30) display low baseline sleep following lights on and preceding lights off. Following SD these flies show

high sleep across time points except following lights on. Flies tend to sleep less as rebound time proceeds. (C) Comparison of sleep lost, baseline sleep, and sleep gain following deprivation at morning and evening timepoints in clock neuron-ablated flies. Morning times are matched with evening time points with similar baselines. Gal4 control flies with no ablated neurons (MB122B> +) (N=29) exhibit greater rebound in the morning compared to the evening time point ($P<0.01$, paired t-test) however exhibit greater sleep lost in the evening ($P<0.01$) and greater baseline sleep during the rebound period ($P<0.05$). Data are means +/- SEM.

Figure 6—figure supplement 1—source data 1

Full SSD demonstrates loss of evening suppression of rebound in LNd ablated flies

Figure 6-figure supplement 2 Silencing LNds and the PDF- sLNv suppresses evening rebound

(A-B) Comparison of sleep lost, baseline sleep, and sleep gain following deprivation at morning and evening timepoints in clock neuron-ablated flies. Morning times are matched with evening time points with similar baselines. (A) Control flies with no silenced neurons (pBDP split > Kir) (N=34) exhibit greater rebound in the morning compared to matched evening time point ($P<0.0001$, paired t-test). (B) Flies with 2-3 LNds and the PDF^- sLNv silenced (MB122B > Kir) (N=31) do not exhibit a significant difference in sleep gain between matched morning/evening time points ($P>0.45$, paired t-test). (C,D) Averaged activity eductions for female flies during the first 2 days of 12:12 LD. Light phase is indicated by white bars while the dark phase is indicated by black bars. Morning and evening anticipation indices are represented in blue and red respectively. (E) Average sleep during the baseline day.(H) 2-3 LNds and the PDF^- sLNv

silenced (MB122B > Kir) (N=31) (green) and control (pBDP split > Kir) (N=34) (purple). Sleep per 24 hours is indicated in the bottom right. Data are means +/- SEM.

Figure 6—figure supplement 2—source data 1

Silencing LNds and the PDF- sLNv suppresses evening rebound

Figure 7-figure supplement 1 Silencing of PPM3, dFB and R5 reduces rebound in the morning and evening

(A, B) Comparison of sleep gain at morning (A) and evening (B) timepoints between flies with silenced neurons (TNTa) and their controls (TNTi). Flies expressing an inactive form of tetanus toxin in PPM3 neurons (R92G05 > TNTi)(N=45) exhibit greater rebound than flies with silenced PPM3 neurons (R92G05 > TNTa)(N=27) in the morning (A) ($P<0.0001$, t-test) and evening (B) ($P<0.0001$, t-test). Flies expressing an inactive form of tetanus toxin in R5 neurons (R58H05 AD; R48H04 DBD > TNTi) (N=21) exhibit greater rebound than flies with R5 neurons silenced (R58H05 AD; R48H04 DBD > TNTa) (N=16) in both the morning (A) ($P<0.0001$, t-test) and evening (B) ($P<0.0001$, t-test). Flies expressing an inactive form of tetanus toxin in the dFB (R23E10 > TNTi) (N=30) than flies with dFB neurons silenced (R23E10 > TNTa)(N=12) in the morning (A) ($P<0.0001$, t-test) and evening (B) ($P<0.0001$, t-test). Data are means +/- SEM.

Figure 7—figure supplement 1—source data 1

Silencing of PPM3, dFB and R5 reduces rebound in the morning and evening

Figure 7-figure supplement 2 Standardized time points show similar effects to points with matched baseline sleep

(A-C) FD sleep during two baseline time periods (sleep lost and baseline sleep) and sleep gain for rebound occurring at ZT1.5 and ZT 9.5.(A) Flies expressing an inactive form of tetanus toxin in PPM3 neurons (R92G05 > TNTi)(N=45) exhibit greater baseline sleep during the rebound period at ZT9.5 ($P<0.001$ paired t-test) and exhibit significantly greater rebound at ZT 1.5 compared to ZT9.5 ($P<0.0001$, paired t-test).(B) Flies with PPM3 neurons silenced with the active form of tetanus toxin (R92G05 > TNTa)(N=27) exhibit significantly less sleep lost ($P<0.05$, paired t-test) and sleep gain ($P<0.0001$, paired t-test) at ZT 9.5 compared to ZT1.5. Data are means +/- SEM.

Figure 7—figure supplement 2—source data 1

Standardized time points show similar effects to points with matched baseline sleep

Figure 8-figure supplement 2 Clock genes are not different between morning and evening in R5 neurons

Scatter plots for core clock genes. Transcripts Per Kilobase Million (TPM) is shown for each sample. All morning samples are grouped, and all evening samples are grouped.

Figure 8—figure supplement 1—source data 1

Clock genes are not different between morning and evening in R5 neurons

Video 1: Flies exhibit sleep following 2.5 hours SD terminating at ZT1.5

Sped up video recording of 4.5 hours of rebound of 36 WT flies following SD from ZT23-ZT1.5. Hours post SD are indicated in red in the bottom right corner. Flies exhibit little movement throughout the 4.5 hours following SD indicating sleep.

Video 2: Flies are active following 2.5 hours SD terminating at ZT9.5

Sped up video recording of 4.5 hours of rebound of 36 WT flies following SD from ZT7-ZT9.5. Hours post SD are indicated in red in the bottom right corner. After a brief period of immobility flies exhibit high activity (low sleep) preceding lights on.

Genotype	Region/Cells targeted	LD morning anticipation	LD evening anticipation	N
+> hid	Clock Gal4 control	0.14 +/- 0.04	0.37 +/- 0.03	17
pBDP split > hid	Split control (HID)	0.13 +/- 0.02	0.24 +/- 0.03	26
pBDP split > kir	Split control (Kir)	0.10 +/- 0.02	0.33 +/-0.04	12
cry39 > hid	broad clock	0.05 +/- 0.02 **	0.12 +/- 0.04 ***	30
pdf > hid	PDF	-0.07 +/- 0.02 ***	0.24 +/- 0.03*	38
cry39*; *pdf-gal80 > hid	LNd and Dn1	0.05 +/- 0.01 *	0.06 +/- 0.04 ***	14
R51H05* AD ; *R18H11* DBD > *hid	Glu+ DN1p	0.06 +/- 0.02 *	0.25 +/- 0.02	22
MB122 > hid	3-4 LNds PDF-sLNv	0.12 +/- 0.02	0.25 +/- 0.02	35
MB122 > kir	3-4 LNds PDF-sLNv	0.07 +/- 0.02	0.22 +/- 0.02	26

Table 1 Summary of male morning and evening anticipation

Data are means +/- SEM (*p<0.05, **p<0.01, ***:p<0.001).

Bibliography

An, W. F., Bowlby, M. R., Betty, M., Cao, J., Ling, H. P., Mendoza, G., . . . Rhodes, K. J. (2000). Modulation of A-type potassium channels by a family of calcium sensors. *Nature, 403*(6769), 553-556. doi:10.1038/35000592

Baines, R. A., Uhler, J. P., Thompson, A., Sweeney, S. T., & Bate, M. (2001). Altered electrical properties in Drosophila neurons developing without synaptic transmission. *J Neurosci, 21*(5), 1523-1531. Retrieved from https://www.ncbi.nlm.nih.gov/pubmed/11222642

Bates, A. S., Manton, J. D., Jagannathan, S. R., Costa, M., Schlegel, P., Rohlfing, T., & Jefferis, G. S. (2020). The natverse, a versatile toolbox for combining and analysing neuroanatomical data. *Elife, 9*. doi:10.7554/eLife.53350

Bates, A. S., Schlegel, P., Roberts, R. J. V., Drummond, N., Tamimi, I. F. M., Turnbull, R., . . . Jefferis, G. (2020). Complete Connectomic Reconstruction of Olfactory Projection Neurons in the Fly Brain. *Curr Biol, 30*(16), 3183-3199 e3186. doi:10.1016/j.cub.2020.06.042

Blum, I. D., Keles, M. F., Baz, E. S., Han, E., Park, K., Luu, S., . . . Wu, M. N. (2021). Astroglial Calcium Signaling Encodes Sleep Need in Drosophila. *Curr Biol, 31*(1), 150-162 e157. doi:10.1016/j.cub.2020.10.012

Borbely, A. A. (1982). A two process model of sleep regulation. *Hum Neurobiol, 1*(3), 195-204. Retrieved from https://www.ncbi.nlm.nih.gov/pubmed/7185792

Borbely, A. A., Daan, S., Wirz-Justice, A., & Deboer, T. (2016). The two-process model of sleep regulation: a reappraisal. *J Sleep Res, 25*(2), 131-143. doi:10.1111/jsr.12371

Bray, N. L., Pimentel, H., Melsted, P., & Pachter, L. (2016). Near-optimal probabilistic RNA-seq quantification. *Nat Biotechnol, 34*(5), 525-527. doi:10.1038/nbt.3519

Broadie, K., Prokop, A., Bellen, H. J., O'Kane, C. J., Schulze, K. L., & Sweeney, S. T. (1995). Syntaxin and synaptobrevin function downstream of vesicle docking in Drosophila. *Neuron, 15*(3), 663-673. doi:10.1016/0896-6273(95)90154-x

Bruning, F., Noya, S. B., Bange, T., Koutsouli, S., Rudolph, J. D., Tyagarajan, S. K., . . . Robles, M. S. (2019). Sleep-wake cycles drive daily dynamics of synaptic phosphorylation. *Science, 366*(6462). doi:10.1126/science.aav3617

Campbell, S. S., & Tobler, I. (1984). Animal sleep: a review of sleep duration across phylogeny. *Neurosci Biobehav Rev, 8*(3), 269-300. doi:10.1016/0149-7634(84)90054-x

Catterall, W. A. (2000). From ionic currents to molecular mechanisms: the structure and function of voltage-gated sodium channels. *Neuron, 26*(1), 13-25. doi:10.1016/s0896-6273(00)81133-2

Cedernaes, J., Huang, W., Ramsey, K. M., Waldeck, N., Cheng, L., Marcheva, B., . . . Bass, J. (2019). Transcriptional Basis for Rhythmic Control of Hunger and Metabolism within the AgRP Neuron. *Cell Metab, 29*(5), 1078-1091 e1075. doi:10.1016/j.cmet.2019.01.023

Chatterjee, A., Lamaze, A., De, J., Mena, W., Chelot, E., Martin, B., . . . Rouyer, F. (2018). Reconfiguration of a Multi-oscillator Network by Light in the Drosophila Circadian Clock. *Curr Biol, 28*(13), 2007-2017 e2004. doi:10.1016/j.cub.2018.04.064

Chen, T. W., Wardill, T. J., Sun, Y., Pulver, S. R., Renninger, S. L., Baohan, A., . . . Kim, D. S. (2013). Ultrasensitive fluorescent proteins for imaging neuronal activity. *Nature, 499*(7458), 295-300. doi:10.1038/nature12354

Chen, X., Rahman, R., Guo, F., & Rosbash, M. (2016). Genome-wide identification of neuronal activity-regulated genes in Drosophila. *Elife, 5*. doi:10.7554/eLife.19942

Chen, Y., Akin, O., Nern, A., Tsui, C. Y., Pecot, M. Y., & Zipursky, S. L. (2014). Cell-type-specific labeling of synapses in vivo through synaptic tagging with recombination. *Neuron, 81*(2), 280-293. doi:10.1016/j.neuron.2013.12.021

Chung, B. Y., Kilman, V. L., Keath, J. R., Pitman, J. L., & Allada, R. (2009). The GABA(A) receptor RDL acts in peptidergic PDF neurons to promote sleep in Drosophila. *Curr Biol, 19*(5), 386-390. doi:10.1016/j.cub.2009.01.040

Collins, B., Pierre-Ferrer, S., Muheim, C., Lukacsovich, D., Cai, Y., Spinnler, A., . . . Brown, S. A. (2020). Circadian VIPergic Neurons of the Suprachiasmatic Nuclei Sculpt the Sleep-Wake Cycle. *Neuron, 108*(3), 486-499 e485. doi:10.1016/j.neuron.2020.08.001

Deboer, T., & Tobler, I. (2000). Slow waves in the sleep electroencephalogram after daily torpor are homeostatically regulated. *Neuroreport, 11*(4), 881-885. doi:10.1097/00001756-200003200-00044

Dijk, D. J., & Czeisler, C. A. (1994). Paradoxical timing of the circadian rhythm of sleep propensity serves to consolidate sleep and wakefulness in humans. *Neurosci Lett, 166*(1), 63-68. doi:10.1016/0304-3940(94)90841-9

Dijk, D. J., & Czeisler, C. A. (1995). Contribution of the circadian pacemaker and the sleep homeostat to sleep propensity, sleep structure, electroencephalographic slow waves, and sleep spindle activity in humans. *J Neurosci, 15*(5 Pt 1), 3526-3538. Retrieved from https://www.ncbi.nlm.nih.gov/pubmed/7751928

Dijk, D. J., & Duffy, J. F. (1999). Circadian regulation of human sleep and age-related changes in its timing, consolidation and EEG characteristics. *Ann Med, 31*(2), 130-140. doi:10.3109/07853899908998789

Dionne, H., Hibbard, K. L., Cavallaro, A., Kao, J. C., & Rubin, G. M. (2018). Genetic Reagents for Making Split-GAL4 Lines in Drosophila. *Genetics, 209*(1), 31-35. doi:10.1534/genetics.118.300682

Donlea, J. M., Pimentel, D., & Miesenbock, G. (2014). Neuronal machinery of sleep homeostasis in Drosophila. *Neuron, 81*(4), 860-872. doi:10.1016/j.neuron.2013.12.013

Donlea, J. M., Thimgan, M. S., Suzuki, Y., Gottschalk, L., & Shaw, P. J. (2011). Inducing sleep by remote control facilitates memory consolidation in Drosophila. *Science, 332*(6037), 1571-1576. doi:10.1126/science.1202249

Dubowy, C., & Sehgal, A. (2017). Circadian Rhythms and Sleep in Drosophila melanogaster. *Genetics, 205*(4), 1373-1397. doi:10.1534/genetics.115.185157

Easton, A., Meerlo, P., Bergmann, B., & Turek, F. W. (2004). The suprachiasmatic nucleus regulates sleep timing and amount in mice. *Sleep, 27*(7), 1307-1318. doi:10.1093/sleep/27.7.1307

Fernandez, R. W., Nurilov, M., Feliciano, O., McDonald, I. S., & Simon, A. F. (2014). Straightforward assay for quantification of social avoidance in Drosophila melanogaster. *J Vis Exp*(94). doi:10.3791/52011

Flourakis, M., Kula-Eversole, E., Hutchison, A. L., Han, T. H., Aranda, K., Moose, D. L., . . . Allada, R. (2015). A Conserved Bicycle Model for Circadian Clock Control of Membrane Excitability. *Cell, 162*(4), 836-848. doi:10.1016/j.cell.2015.07.036

Franken, P., Dijk, D. J., Tobler, I., & Borbely, A. A. (1991). Sleep deprivation in rats: effects on EEG power spectra, vigilance states, and cortical temperature. *Am J Physiol, 261*(1 Pt 2), R198-208. doi:10.1152/ajpregu.1991.261.1.R198

Franken, P., Dudley, C. A., Estill, S. J., Barakat, M., Thomason, R., O'Hara, B. F., & McKnight, S. L. (2006). NPAS2 as a transcriptional regulator of non-rapid eye movement sleep: genotype and sex interactions. *Proc Natl Acad Sci U S A, 103*(18), 7118-7123. doi:10.1073/pnas.0602006103

Gilestro, G. F., Tononi, G., & Cirelli, C. (2009). Widespread changes in synaptic markers as a function of sleep and wakefulness in Drosophila. *Science, 324*(5923), 109-112. doi:10.1126/science.1166673

Gossan, N. C., Zhang, F., Guo, B., Jin, D., Yoshitane, H., Yao, A., . . . Meng, Q. J. (2014). The E3 ubiquitin ligase UBE3A is an integral component of the molecular circadian clock through regulating the BMAL1 transcription factor. *Nucleic Acids Res, 42*(9), 5765-5775. doi:10.1093/nar/gku225

Grima, B., Chelot, E., Xia, R., & Rouyer, F. (2004). Morning and evening peaks of activity rely on different clock neurons of the Drosophila brain. *Nature, 431*(7010), 869-873. doi:10.1038/nature02935

Guo, F., Chen, X., & Rosbash, M. (2017). Temporal calcium profiling of specific circadian neurons in freely moving flies. *Proc Natl Acad Sci U S A, 114*(41), E8780-E8787. doi:10.1073/pnas.1706608114

Guo, F., Holla, M., Diaz, M. M., & Rosbash, M. (2018). A Circadian Output Circuit Controls Sleep-Wake Arousal in Drosophila. *Neuron, 100*(3), 624-635 e624. doi:10.1016/j.neuron.2018.09.002

Guo, F., Yu, J., Jung, H. J., Abruzzi, K. C., Luo, W., Griffith, L. C., & Rosbash, M. (2016). Circadian neuron feedback controls the Drosophila sleep--activity profile. *Nature, 536*(7616), 292-297. doi:10.1038/nature19097

Hamblencoyle, M. J., Wheeler, D. A., Rutila, J. E., Rosbash, M., & Hall, J. C. (1992). Behavior of Period-Altered Circadian-Rhythm Mutants of Drosophila in Light - Dark Cycles (Diptera, Drosophilidae). *Journal of Insect Behavior, 5*(4), 417-446. doi:Doi 10.1007/Bf01058189

Haug-Collet, K., Pearson, B., Webel, R., Szerencsei, R. T., Winkfein, R. J., Schnetkamp, P. P., & Colley, N. J. (1999). Cloning and characterization of a potassium-dependent sodium/calcium exchanger in Drosophila. *J Cell Biol, 147*(3), 659-670. doi:10.1083/jcb.147.3.659

Hendricks, J. C., Finn, S. M., Panckeri, K. A., Chavkin, J., Williams, J. A., Sehgal, A., & Pack, A. I. (2000). Rest in Drosophila is a sleep-like state. *Neuron, 25*(1), 129-138. doi:10.1016/s0896-6273(00)80877-6

Huang, S., Piao, C., Beuschel, C. B., Gotz, T., & Sigrist, S. J. (2020). Presynaptic Active Zone Plasticity Encodes Sleep Need in Drosophila. *Curr Biol, 30*(6), 1077-1091 e1075. doi:10.1016/j.cub.2020.01.019

Huber, R., Hill, S. L., Holladay, C., Biesiadecki, M., Tononi, G., & Cirelli, C. (2004). Sleep homeostasis in Drosophila melanogaster. *Sleep, 27*(4), 628-639. doi:10.1093/sleep/27.4.628

Isaac, R. E., Li, C., Leedale, A. E., & Shirras, A. D. (2010). Drosophila male sex peptide inhibits siesta sleep and promotes locomotor activity in the post-mated female. *Proc Biol Sci, 277*(1678), 65-70. doi:10.1098/rspb.2009.1236

Iyer, S. C., Ramachandran Iyer, E. P., Meduri, R., Rubaharan, M., Kuntimaddi, A., Karamsetty, M., & Cox, D. N. (2013). Cut, via CrebA, transcriptionally regulates the COPII secretory pathway to direct dendrite development in Drosophila. *J Cell Sci, 126*(Pt 20), 4732-4745. doi:10.1242/jcs.131144

Jenett, A., Rubin, G. M., Ngo, T. T., Shepherd, D., Murphy, C., Dionne, H., . . . Zugates, C. T. (2012). A GAL4-driver line resource for Drosophila neurobiology. *Cell Rep, 2*(4), 991-1001. doi:10.1016/j.celrep.2012.09.011

Johnson, E. L., 3rd, Fetter, R. D., & Davis, G. W. (2009). Negative regulation of active zone assembly by a newly identified SR protein kinase. *PLoS Biol, 7*(9), e1000193. doi:10.1371/journal.pbio.1000193

Kayser, M. S., Yue, Z., & Sehgal, A. (2014). A critical period of sleep for development of courtship circuitry and behavior in Drosophila. *Science, 344*(6181), 269-274. doi:10.1126/science.1250553

Klarsfeld, A., Malpel, S., Michard-Vanhee, C., Picot, M., Chelot, E., & Rouyer, F. (2004). Novel features of cryptochrome-mediated photoreception in the brain circadian clock of Drosophila. *J Neurosci, 24*(6), 1468-1477. doi:10.1523/JNEUROSCI.3661-03.2004

Konopka, R. J., & Benzer, S. (1971). Clock mutants of Drosophila melanogaster. *Proc Natl Acad Sci U S A, 68*(9), 2112-2116. doi:10.1073/pnas.68.9.2112

Kunst, M., Hughes, M. E., Raccuglia, D., Felix, M., Li, M., Barnett, G., . . . Nitabach, M. N. (2014). Calcitonin gene-related peptide neurons mediate sleep-specific circadian output in Drosophila. *Curr Biol, 24*(22), 2652-2664. doi:10.1016/j.cub.2014.09.077

1237 Lamaze, A., Kratschmer, P., Chen, K. F., Lowe, S., & Jepson, J. E. C. (2018). A Wake-
1238 Promoting Circadian Output Circuit in Drosophila. *Curr Biol, 28*(19), 3098-3105 e3093.
1239 doi:10.1016/j.cub.2018.07.024
1240 Laposky, A., Easton, A., Dugovic, C., Walisser, J., Bradfield, C., & Turek, F. (2005). Deletion of
1241 the mammalian circadian clock gene BMAL1/Mop3 alters baseline sleep architecture
1242 and the response to sleep deprivation. *Sleep, 28*(4), 395-409.
1243 doi:10.1093/sleep/28.4.395
1244 Lazar, A. S., Lazar, Z. I., & Dijk, D. J. (2015). Circadian regulation of slow waves in human
1245 sleep: Topographical aspects. *Neuroimage, 116*, 123-134.
1246 doi:10.1016/j.neuroimage.2015.05.012
1247 Lee, E., Jeong, E. H., Jeong, H. J., Yildirim, E., Vanselow, J. T., Ng, F., . . . Kim, E. Y. (2014).
1248 Phosphorylation of a central clock transcription factor is required for thermal but not
1249 photic entrainment. *PLoS Genet, 10*(8), e1004545. doi:10.1371/journal.pgen.1004545
1250 Lee, P. T., Lin, G., Lin, W. W., Diao, F., White, B. H., & Bellen, H. J. (2018). A kinase-dependent
1251 feedforward loop affects CREBB stability and long term memory formation. *Elife, 7*.
1252 doi:10.7554/eLife.33007
1253 Liang, X., Ho, M. C. W., Zhang, Y., Li, Y., Wu, M. N., Holy, T. E., & Taghert, P. H. (2019).
1254 Morning and Evening Circadian Pacemakers Independently Drive Premotor Centers via
1255 a Specific Dopamine Relay. *Neuron, 102*(4), 843-857 e844.
1256 doi:10.1016/j.neuron.2019.03.028
1257 Liang, X., Holy, T. E., & Taghert, P. H. (2017). A Series of Suppressive Signals within the
1258 Drosophila Circadian Neural Circuit Generates Sequential Daily Outputs. *Neuron, 94*(6),
1259 1173-1189 e1174. doi:10.1016/j.neuron.2017.05.007
1260 Liu, S., Liu, Q., Tabuchi, M., & Wu, M. N. (2016). Sleep Drive Is Encoded by Neural Plastic
1261 Changes in a Dedicated Circuit. *Cell, 165*(6), 1347-1360. doi:10.1016/j.cell.2016.04.013
1262 Loughney, K., Kreber, R., & Ganetzky, B. (1989). Molecular analysis of the para locus, a sodium
1263 channel gene in Drosophila. *Cell, 58*(6), 1143-1154. doi:10.1016/0092-8674(89)90512-6
1264 Lovick, J. K., Omoto, J. J., Ngo, K. T., & Hartenstein, V. (2017). Development of the anterior
1265 visual input pathway to the Drosophila central complex. *J Comp Neurol, 525*(16), 3458-
1266 3475. doi:10.1002/cne.24277
1267 Matkovic, T., Siebert, M., Knoche, E., Depner, H., Mertel, S., Owald, D., . . . Sigrist, S. J. (2013).
1268 The Bruchpilot cytomatrix determines the size of the readily releasable pool of synaptic
1269 vesicles. *J Cell Biol, 202*(4), 667-683. doi:10.1083/jcb.201301072
1270 Miyasako, Y., Umezaki, Y., & Tomioka, K. (2007). Separate sets of cerebral clock neurons are
1271 responsible for light and temperature entrainment of Drosophila circadian locomotor
1272 rhythms. *J Biol Rhythms, 22*(2), 115-126. doi:10.1177/0748730407299344
1273 Muller, M., Liu, K. S., Sigrist, S. J., & Davis, G. W. (2012). RIM controls homeostatic plasticity
1274 through modulation of the readily-releasable vesicle pool. *J Neurosci, 32*(47), 16574-
1275 16585. doi:10.1523/JNEUROSCI.0981-12.2012
1276 Nall, A. H., & Sehgal, A. (2013). Small-molecule screen in adult Drosophila identifies VMAT as a
1277 regulator of sleep. *J Neurosci, 33*(19), 8534-8540. doi:10.1523/JNEUROSCI.0253-
1278 13.2013
1279 Ni, J. D., Gurav, A. S., Liu, W., Ogunmowo, T. H., Hackbart, H., Elsheikh, A., . . . Montell, C.
1280 (2019). Differential regulation of the Drosophila sleep homeostat by circadian and
1281 arousal inputs. *Elife, 8*. doi:10.7554/eLife.40487
1282 Nicolai, L. J., Ramaekers, A., Raemaekers, T., Drozdzecki, A., Mauss, A. S., Yan, J., . . .
1283 Hassan, B. A. (2010). Genetically encoded dendritic marker sheds light on neuronal
1284 connectivity in Drosophila. *Proc Natl Acad Sci U S A, 107*(47), 20553-20558.
1285 doi:10.1073/pnas.1010198107
1286 Nieratschker, V., Schubert, A., Jauch, M., Bock, N., Bucher, D., Dippacher, S., . . . Buchner, E.
1287 (2009). Bruchpilot in ribbon-like axonal agglomerates, behavioral defects, and early

death in SRPK79D kinase mutants of Drosophila. *PLoS Genet, 5*(10), e1000700. doi:10.1371/journal.pgen.1000700

Noya, S. B., Colameo, D., Bruning, F., Spinnler, A., Mircsof, D., Opitz, L., . . . Brown, S. A. (2019). The forebrain synaptic transcriptome is organized by clocks but its proteome is driven by sleep. *Science, 366*(6462). doi:10.1126/science.aav2642

Oh, Y., Yoon, S. E., Zhang, Q., Chae, H. S., Daubnerova, I., Shafer, O. T., . . . Kim, Y. J. (2014). A homeostatic sleep-stabilizing pathway in Drosophila composed of the sex peptide receptor and its ligand, the myoinhibitory peptide. *PLoS Biol, 12*(10), e1001974. doi:10.1371/journal.pbio.1001974

Omoto, J. J., Keles, M. F., Nguyen, B. M., Bolanos, C., Lovick, J. K., Frye, M. A., & Hartenstein, V. (2017). Visual Input to the Drosophila Central Complex by Developmentally and Functionally Distinct Neuronal Populations. *Curr Biol, 27*(8), 1098-1110. doi:10.1016/j.cub.2017.02.063

Parisky, K. M., Agosto, J., Pulver, S. R., Shang, Y., Kuklin, E., Hodge, J. J., . . . Griffith, L. C. (2008). PDF cells are a GABA-responsive wake-promoting component of the Drosophila sleep circuit. *Neuron, 60*(4), 672-682. doi:10.1016/j.neuron.2008.10.042

Patke, A., Young, M. W., & Axelrod, S. (2020). Molecular mechanisms and physiological importance of circadian rhythms. *Nat Rev Mol Cell Biol, 21*(2), 67-84. doi:10.1038/s41580-019-0179-2

Pfeiffenberger, C., & Allada, R. (2012). Cul3 and the BTB adaptor insomniac are key regulators of sleep homeostasis and a dopamine arousal pathway in Drosophila. *PLoS Genet, 8*(10), e1003003. doi:10.1371/journal.pgen.1003003

Pfeiffenberger, C., Lear, B. C., Keegan, K. P., & Allada, R. (2010a). Processing circadian data collected from the Drosophila Activity Monitoring (DAM) System. *Cold Spring Harb Protoc, 2010*(11), pdb prot5519. doi:10.1101/pdb.prot5519

Pfeiffenberger, C., Lear, B. C., Keegan, K. P., & Allada, R. (2010b). Processing sleep data created with the Drosophila Activity Monitoring (DAM) System. *Cold Spring Harb Protoc, 2010*(11), pdb prot5520. doi:10.1101/pdb.prot5520

Picot, M., Cusumano, P., Klarsfeld, A., Ueda, R., & Rouyer, F. (2007). Light activates output from evening neurons and inhibits output from morning neurons in the Drosophila circadian clock. *PLoS Biol, 5*(11), e315. doi:10.1371/journal.pbio.0050315

Pimentel, H., Bray, N. L., Puente, S., Melsted, P., & Pachter, L. (2017). Differential analysis of RNA-seq incorporating quantification uncertainty. *Nat Methods, 14*(7), 687-690. doi:10.1038/nmeth.4324

Qian, Y., Cao, Y., Deng, B., Yang, G., Li, J., Xu, R., . . . Rao, Y. (2017). Sleep homeostasis regulated by 5HT2b receptor in a small subset of neurons in the dorsal fan-shaped body of drosophila. *Elife, 6*. doi:10.7554/eLife.26519

Raccuglia, D., Huang, S., Ender, A., Heim, M. M., Laber, D., Suarez-Grimalt, R., . . . Owald, D. (2019). Network-Specific Synchronization of Electrical Slow-Wave Oscillations Regulates Sleep Drive in Drosophila. *Curr Biol, 29*(21), 3611-3621 e3613. doi:10.1016/j.cub.2019.08.070

Scheffer, L. K., Xu, C. S., Januszewski, M., Lu, Z., Takemura, S. Y., Hayworth, K. J., . . . Plaza, S. M. (2020). A connectome and analysis of the adult Drosophila central brain. *Elife, 9*. doi:10.7554/eLife.57443

Schubert, F. K., Hagedorn, N., Yoshii, T., Helfrich-Forster, C., & Rieger, D. (2018). Neuroanatomical details of the lateral neurons of Drosophila melanogaster support their functional role in the circadian system. *J Comp Neurol, 526*(7), 1209-1231. doi:10.1002/cne.24406

Shafer, O. T., & Keene, A. C. (2021). The Regulation of Drosophila Sleep. *Curr Biol, 31*(1), R38-R49. doi:10.1016/j.cub.2020.10.082

Shaw, P. J., Cirelli, C., Greenspan, R. J., & Tononi, G. (2000). Correlates of sleep and waking in Drosophila melanogaster. *Science, 287*(5459), 1834-1837. doi:10.1126/science.287.5459.1834

Shaw, P. J., Tononi, G., Greenspan, R. J., & Robinson, D. F. (2002). Stress response genes protect against lethal effects of sleep deprivation in Drosophila. *Nature, 417*(6886), 287-291. doi:10.1038/417287a

Sheeba, V., Fogle, K. J., Kaneko, M., Rashid, S., Chou, Y. T., Sharma, V. K., & Holmes, T. C. (2008). Large ventral lateral neurons modulate arousal and sleep in Drosophila. *Curr Biol, 18*(20), 1537-1545. doi:10.1016/j.cub.2008.08.033

Sisobhan, S., Rosensweig, C., Lear, B. C., & Allada, R. (2022). SleepMat: A New Behavioral Analysis Software Program for Sleep and Circadian Rhythms. *bioRxiv*, 2022.2001.2031.478545. doi:10.1101/2022.01.31.478545

Stoleru, D., Peng, Y., Agosto, J., & Rosbash, M. (2004). Coupled oscillators control morning and evening locomotor behaviour of Drosophila. *Nature, 431*(7010), 862-868. doi:10.1038/nature02926

Tobler, I., Borbely, A. A., & Groos, G. (1983). The effect of sleep deprivation on sleep in rats with suprachiasmatic lesions. *Neurosci Lett, 42*(1), 49-54. doi:10.1016/0304-3940(83)90420-2

Tononi, G., & Cirelli, C. (2014). Sleep and the price of plasticity: from synaptic and cellular homeostasis to memory consolidation and integration. *Neuron, 81*(1), 12-34. doi:10.1016/j.neuron.2013.12.025

Vaccaro, A., Kaplan Dor, Y., Nambara, K., Pollina, E. A., Lin, C., Greenberg, M. E., & Rogulja, D. (2020). Sleep Loss Can Cause Death through Accumulation of Reactive Oxygen Species in the Gut. *Cell, 181*(6), 1307-1328 e1315. doi:10.1016/j.cell.2020.04.049

van Alphen, B., Yap, M. H., Kirszenblat, L., Kottler, B., & van Swinderen, B. (2013). A dynamic deep sleep stage in Drosophila. *J Neurosci, 33*(16), 6917-6927. doi:10.1523/JNEUROSCI.0061-13.2013

Werth, E., Dijk, D. J., Achermann, P., & Borbely, A. A. (1996). Dynamics of the sleep EEG after an early evening nap: experimental data and simulations. *Am J Physiol, 271*(3 Pt 2), R501-510. doi:10.1152/ajpregu.1996.271.3.R501

Wisor, J. P., O'Hara, B. F., Terao, A., Selby, C. P., Kilduff, T. S., Sancar, A., . . . Franken, P. (2002). A role for cryptochromes in sleep regulation. *BMC Neurosci, 3*, 20. doi:10.1186/1471-2202-3-20

Xu, F., Kula-Eversole, E., Iwanaszko, M., Lim, C., & Allada, R. (2019). Ataxin2 functions via CrebA to mediate Huntingtin toxicity in circadian clock neurons. *PLoS Genet, 15*(10), e1008356. doi:10.1371/journal.pgen.1008356

Yin, J. C., Del Vecchio, M., Zhou, H., & Tully, T. (1995). CREB as a memory modulator: induced expression of a dCREB2 activator isoform enhances long-term memory in Drosophila. *Cell, 81*(1), 107-115. doi:10.1016/0092-8674(95)90375-5

Zhang, L., Chung, B. Y., Lear, B. C., Kilman, V. L., Liu, Y., Mahesh, G., . . . Allada, R. (2010). DN1(p) circadian neurons coordinate acute light and PDF inputs to produce robust daily behavior in Drosophila. *Curr Biol, 20*(7), 591-599. doi:10.1016/j.cub.2010.02.056

Zhang, Y., Liu, Y., Bilodeau-Wentworth, D., Hardin, P. E., & Emery, P. (2010). Light and temperature control the contribution of specific DN1 neurons to Drosophila circadian behavior. *Curr Biol, 20*(7), 600-605. doi:10.1016/j.cub.2010.02.044

Zhang, Y. Q., Rodesch, C. K., & Broadie, K. (2002). Living synaptic vesicle marker: synaptotagmin-GFP. *Genesis, 34*(1-2), 142-145. doi:10.1002/gene.10144

Zhang, Y. V., Hannan, S. B., Kern, J. V., Stanchev, D. T., Koc, B., Jahn, T. R., & Rasse, T. M. (2017). The KIF1A homolog Unc-104 is important for spontaneous release, postsynaptic density maturation and perisynaptic scaffold organization. *Sci Rep, 7*, 38172. doi:10.1038/srep38172

1389

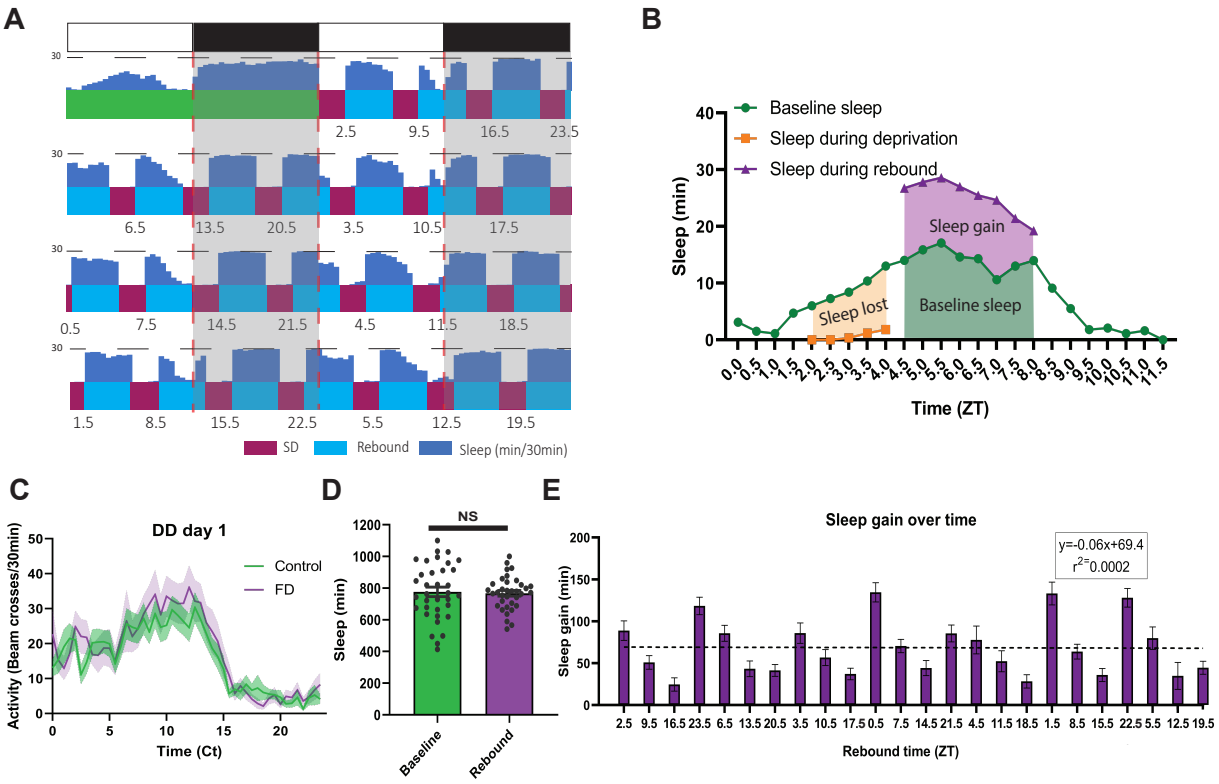
A
B
C
D
E
SD
Rebound
Sleep (min/30min)
Baseline sleep
Sleep during deprivation
Sleep during rebound
Sleep gain
Sleep lost
Baseline sleep
Sleep (min)
Time (ZT)
DD day 1
Control
FD
Activity (Beam crosses/30min)
Time (Ct)
NS
Sleep (min)
Baseline
Rebound
Sleep gain over time
y=-0.06x+69.4
r2=0.0002
Sleep gain (min)
Rebound time (ZT)

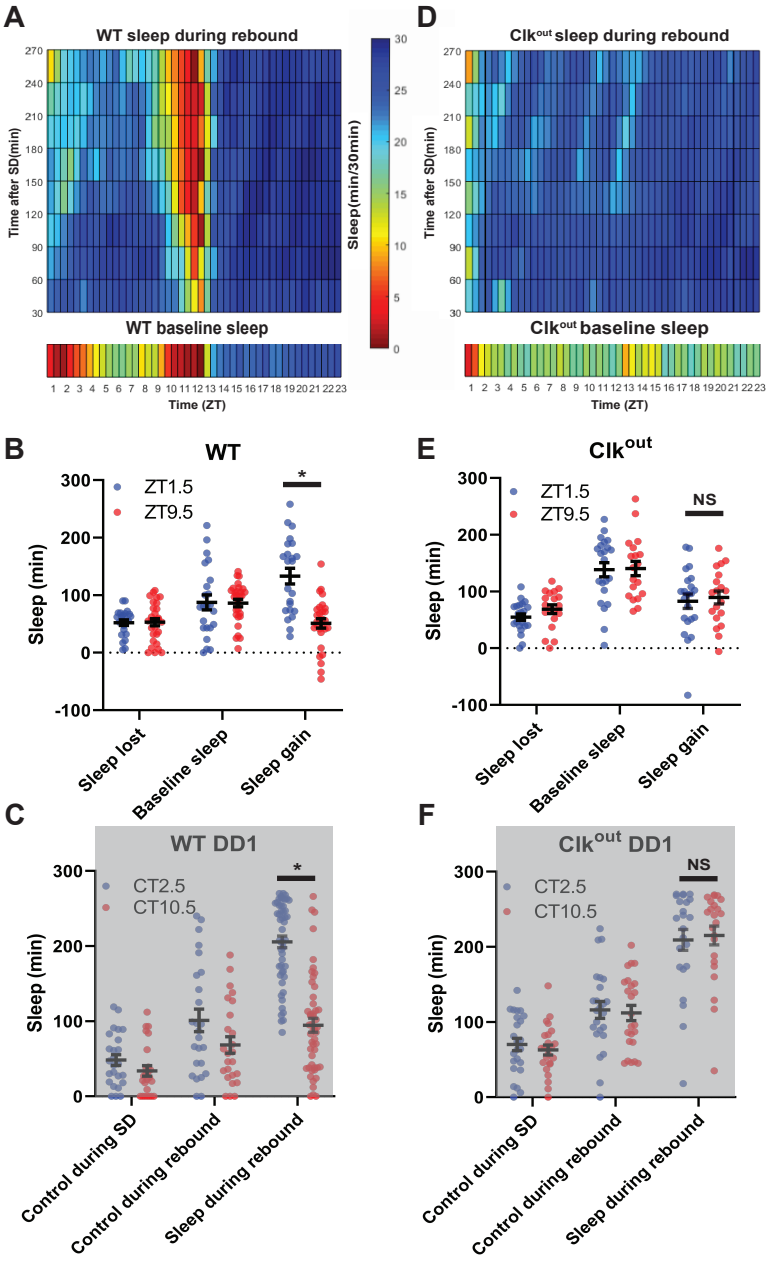
A
WT sleep during rebound
Time after SD(min)
Sleep(min/30min)
WT baseline sleep
Time (ZT)
D
Clk^out sleep during rebound
Clk^out baseline sleep
B
WT
ZT1.5
ZT9.5
Sleep (min)
Sleep lost
Baseline sleep
Sleep gain
E
Clk^out
NS
C
WT DD1
CT2.5
CT10.5
Control during SD
Control during rebound
Sleep during rebound
F
Clk^out DD1

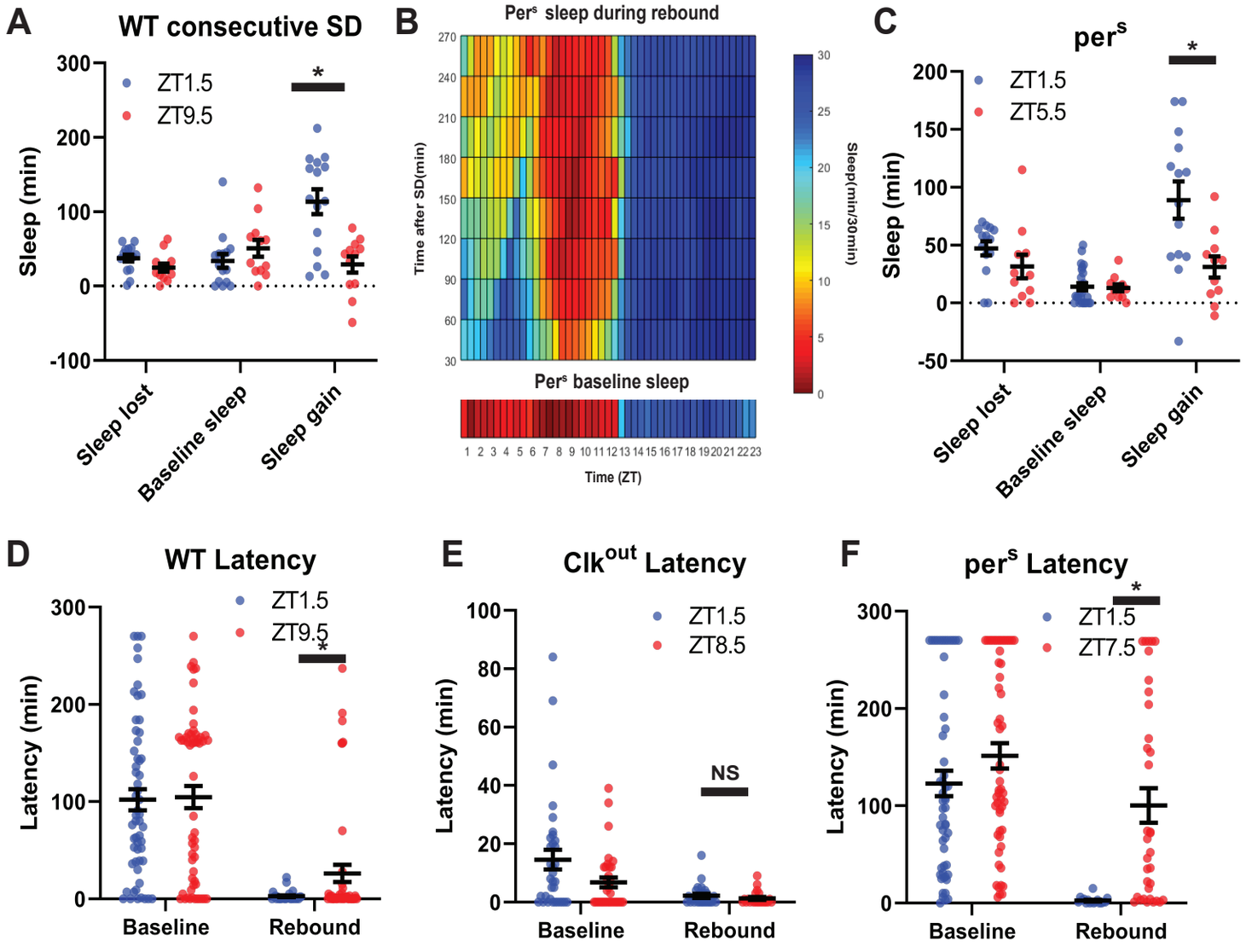
A
WT consecutive SD
Sleep (min)
ZT1.5
ZT9.5
*
Sleep lost
Baseline sleep
Sleep gain
B
Per^{s} sleep during rebound
Time after SD(min)
Per^{s} baseline sleep
Time (ZT)
Sleep(min/30min)
C
per^{s}
ZT1.5
ZT5.5
Sleep (min)
D
WT Latency
Latency (min)
Baseline
Rebound
E
Clk^{out} Latency
ZT8.5
NS
F
per^{s} Latency
ZT7.5

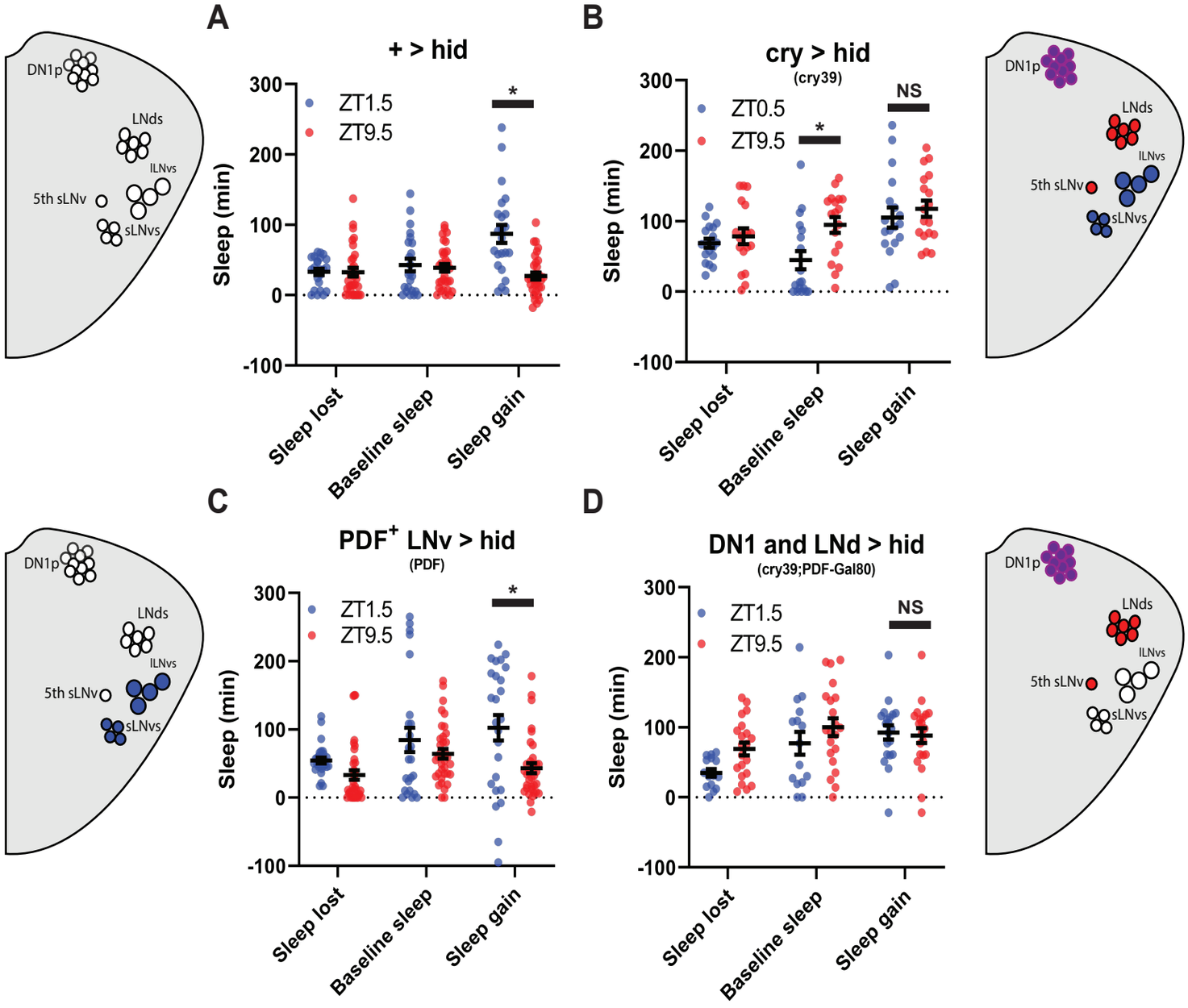
A
+ > hid
ZT1.5
ZT9.5
*
Sleep (min)
300
200
100
0
-100
Sleep lost
Baseline sleep
Sleep gain
DN1p
LNds
lLNvs
5th sLNv
sLNvs
B
cry > hid
(cry39)
ZT0.5
ZT9.5
*
NS
C
PDF+ LNv > hid
(PDF)
D
DN1 and LNd > hid
(cry39;PDF-Gal80)

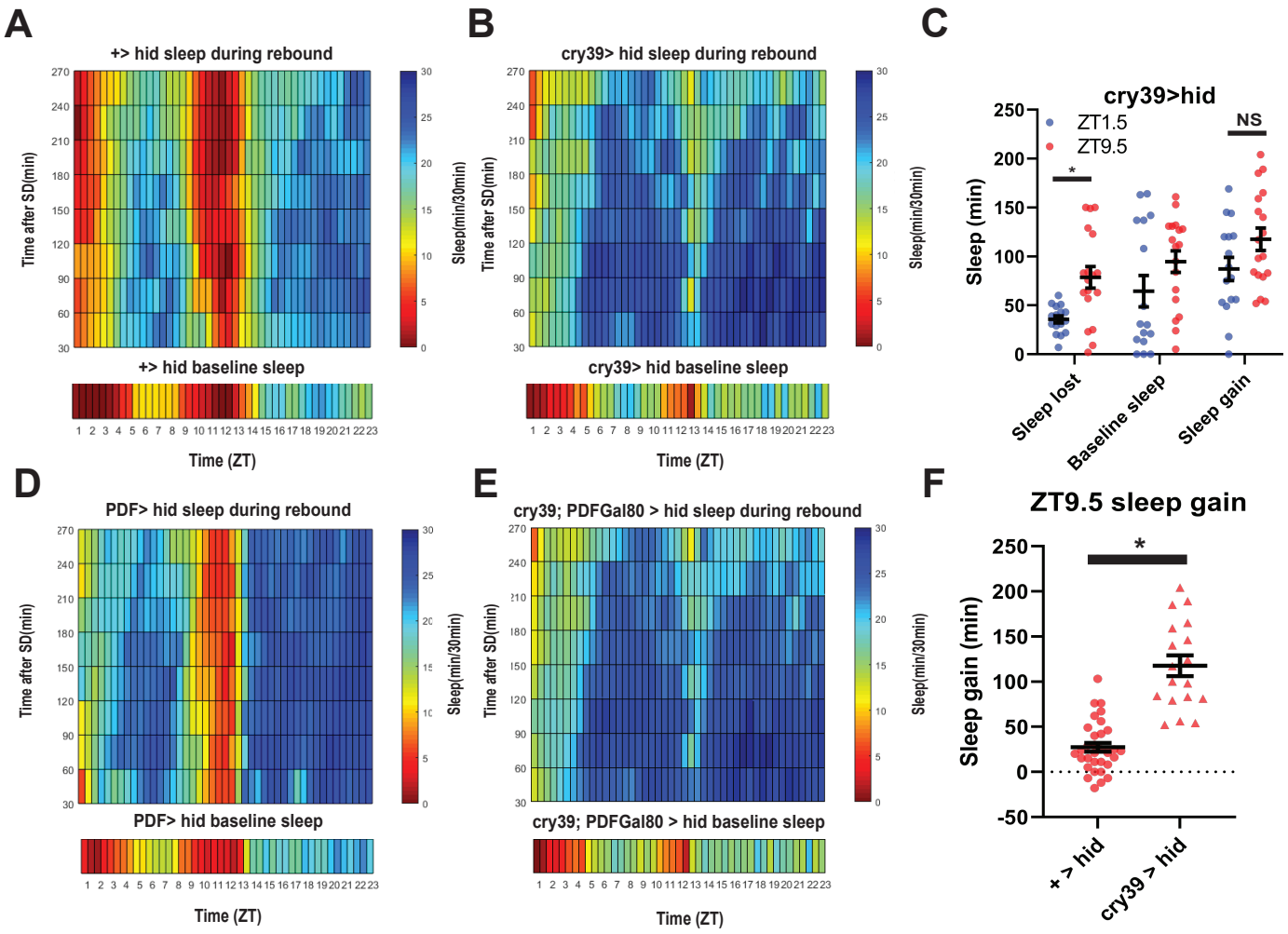
A
+> hid sleep during rebound
Time after SD(min)
Sleep(min/30min)
+> hid baseline sleep
Time (ZT)
B
cry39> hid sleep during rebound
cry39> hid baseline sleep
Time (ZT)
C
cry39>hid
ZT1.5
ZT9.5
NS
*
Sleep (min)
Sleep lost
Baseline sleep
Sleep gain
D
PDF> hid sleep during rebound
PDF> hid baseline sleep
Time (ZT)
E
cry39; PDFGal80 > hid sleep during rebound
cry39; PDFGal80 > hid baseline sleep
Time (ZT)
F
ZT9.5 sleep gain
Sleep gain (min)
+ > hid
cry39 > hid

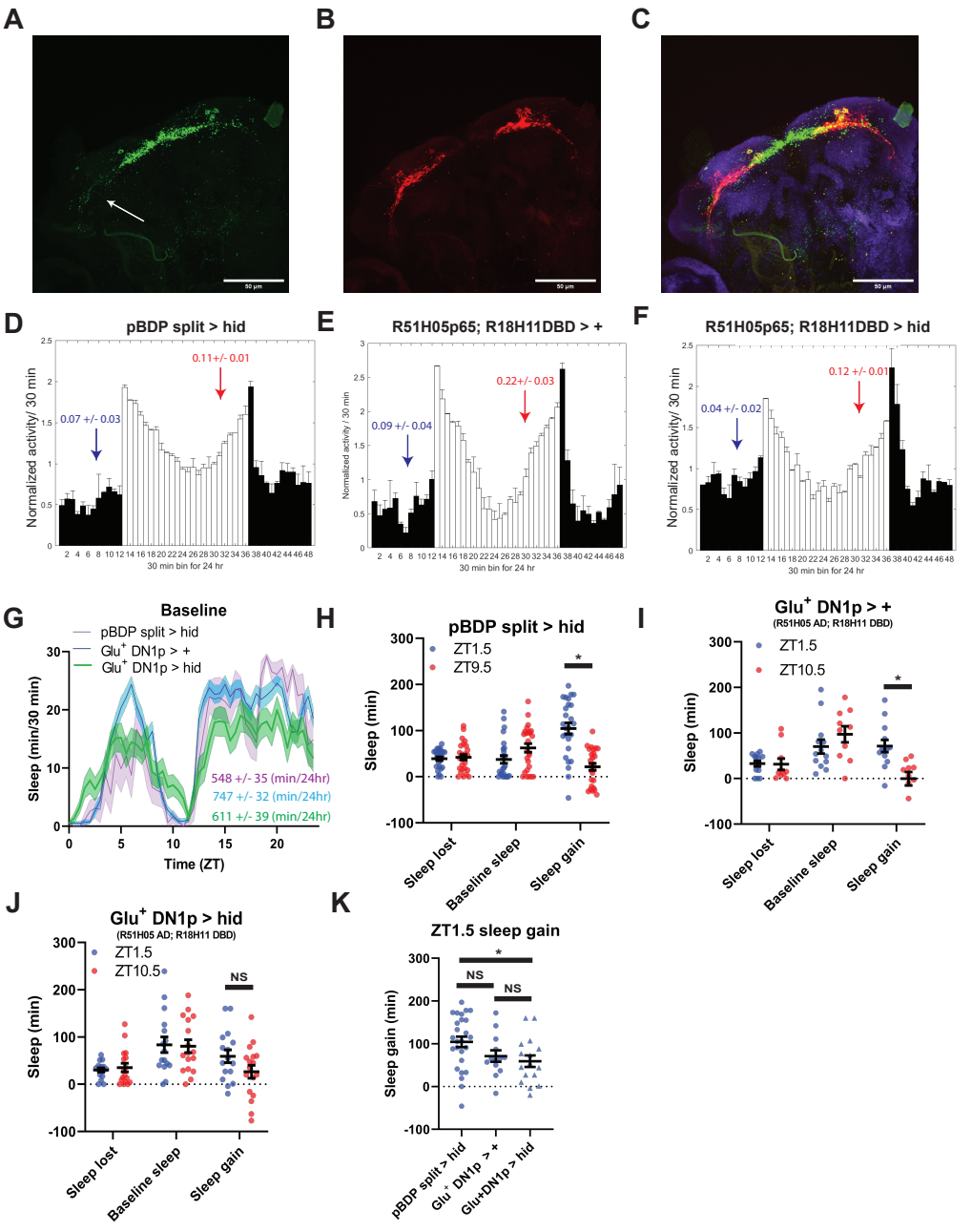
A
B
C
D
pBDP split > hid
0.07 +/- 0.03
0.11+/- 0.01
Normalized activity/ 30 min
30 min bin for 24 hr
E
R51H05p65; R18H11DBD > +
0.09 +/- 0.04
0.22+/- 0.03
Normalized activity / 30 min
30 min bin for 24 hr
F
R51H05p65; R18H11DBD > hid
0.04 +/- 0.02
0.12 +/- 0.01
Normalized activity/ 30 min
30 min bin for 24 hr
G
Baseline
pBDP split > hid
Glu+ DN1p > +
Glu+ DN1p > hid
548 +/- 35 (min/24hr)
747 +/- 32 (min/24hr)
611 +/- 39 (min/24hr)
Sleep (min/30 min)
Time (ZT)
H
pBDP split > hid
ZT1.5
ZT9.5
Sleep (min)
Sleep lost
Baseline sleep
Sleep gain
I
Glu+ DN1p > +
(R51H05 AD; R18H11 DBD)
ZT1.5
ZT10.5
Sleep (min)
Sleep lost
Baseline sleep
Sleep gain
J
Glu+ DN1p > hid
(R51H05 AD; R18H11 DBD)
ZT1.5
ZT10.5
NS
Sleep (min)
Sleep lost
Baseline sleep
Sleep gain
K
ZT1.5 sleep gain
NS
NS
Sleep gain (min)
pBDP split > hid
Glu+ DN1p > +
Glu+DN1p > hid

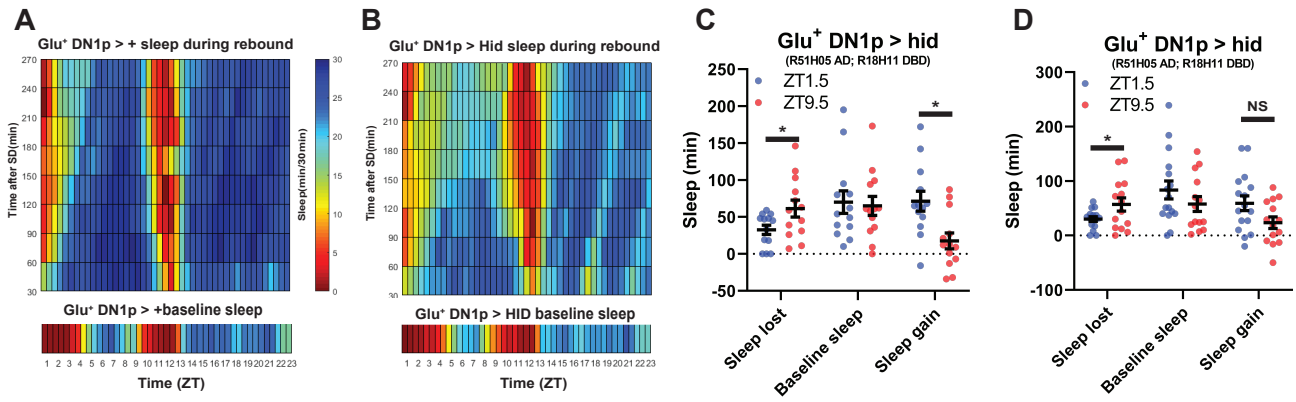
A
Glu+ DN1p > + sleep during rebound
Time after SD(min)
Sleep(min/30min)
Glu+ DN1p > +baseline sleep
Time (ZT)
B
Glu+ DN1p > Hid sleep during rebound
Time after SD(min)
Glu+ DN1p > HID baseline sleep
Time (ZT)
C
Glu+ DN1p > hid
(R51H05 AD; R18H11 DBD)
ZT1.5
ZT9.5
Sleep (min)
Sleep lost
Baseline sleep
Sleep gain
D
Glu+ DN1p > hid
(R51H05 AD; R18H11 DBD)
ZT1.5
ZT9.5
NS
Sleep (min)
Sleep lost
Baseline sleep
Sleep gain

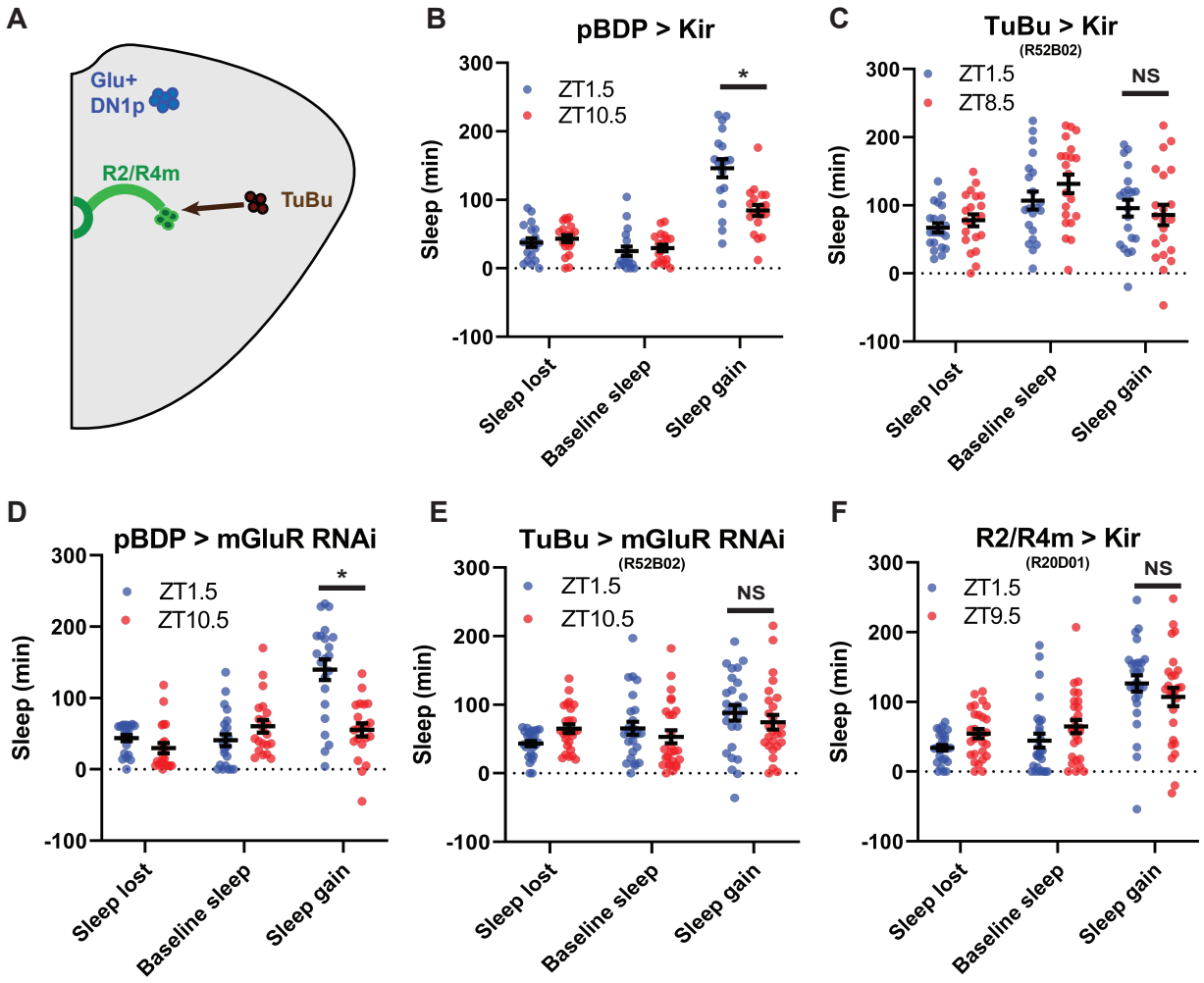

Figure 5: TuBu intermediates convey enhanced morning glutamatergic signal to R2/R4m ellipsoid body neurons

(A) Cartoon illustrating proposed link between Glu+ DN1ps and R2/R4m with Tubu intermediates. (B-F) Comparison of sleep lost, baseline sleep, and sleep gain following deprivation at morning and evening timepoints while modulating neurons linking DN1ps to the EB. Morning times are matched with evening time points with similar baselines. (B) Enhancerless-Gal4 control flies (pBDP > Kir) (N=21) exhibit greater rebound in the morning compared to a matched evening time point ($P<0.01$, paired t-test). (C) Flies with TuBu neurons silenced (R52B02 > Kir) (N=21) do not exhibit a difference in rebound between matched morning/evening time points($P> 0.38$, paired t-test). (D) Enhancerless-Gal4 driver paired with UAS-GluR-RNAi (pBDP > GluR RNAi) control (N=32) exhibit greater rebound in the morning compared to matched evening time point ($P<0.00001$, paired t-test). (E) Flies with KD of GluR in TuBu neurons (R52B02 > GluR RNAi) do not exhibit a significant difference between matched morning/evening time points ($P>0.28$, paired t-test). (F) Flies with R2/R4m neurons silenced (R20D01 > Kir) (N=32) do not exhibit a significant difference in rebound between matched morning/evening time points($P>0.26$, paired t-test). Data are means +/- SEM.

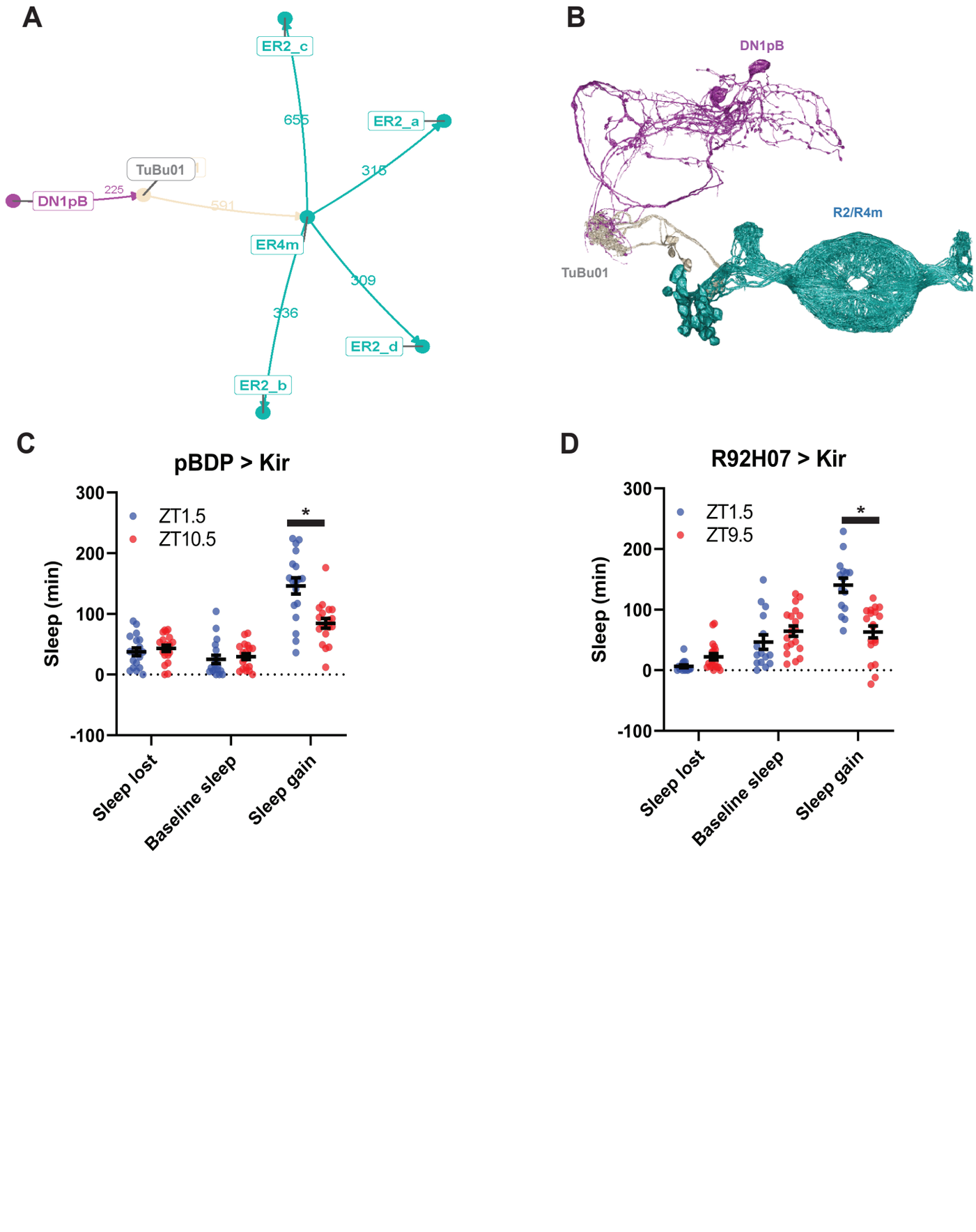
A
ER2_c
655
ER2_a
TuBu01
315
225
DN1pB
591
ER4m
309
336
ER2_d
ER2_b
B
DN1pB
R2/R4m
TuBu01
C
pBDP > Kir
ZT1.5
ZT10.5
*
Sleep (min)
300
200
100
0
-100
Sleep lost
Baseline sleep
Sleep gain
D
R92H07 > Kir
ZT1.5
ZT9.5
*
Sleep (min)
300
200
100
0
-100
Sleep lost
Baseline sleep
Sleep gain

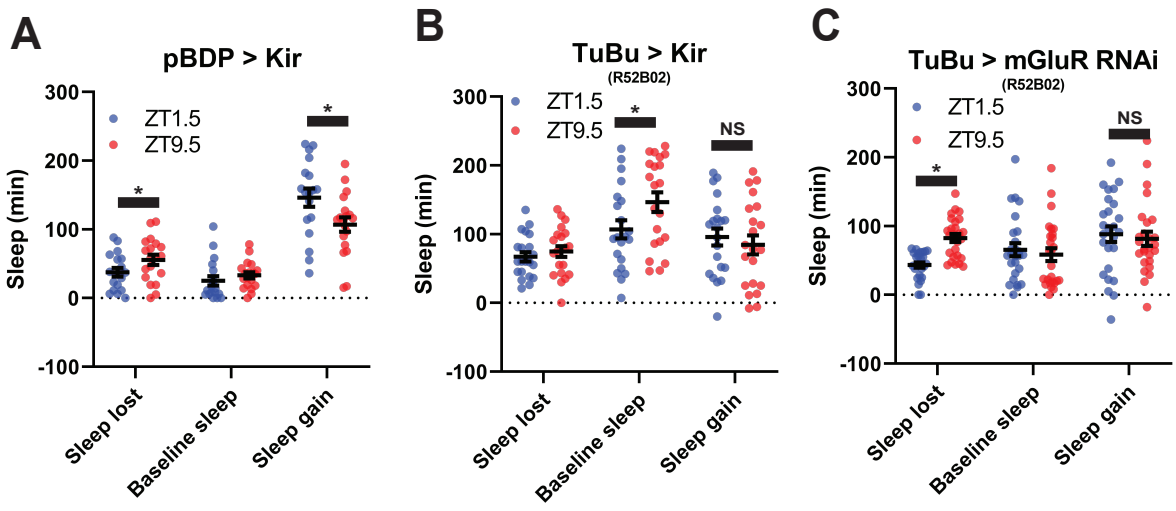
A
pBDP > Kir
ZT1.5
ZT9.5
Sleep (min)
300
200
100
0
-100
*
*
Sleep lost
Baseline sleep
Sleep gain
B
TuBu > Kir
(R52B02)
ZT1.5
ZT9.5
Sleep (min)
300
200
100
0
-100
*
NS
Sleep lost
Baseline sleep
Sleep gain
C
TuBu > mGluR RNAi
(R52B02)
ZT1.5
ZT9.5
Sleep (min)
300
200
100
0
-100
*
NS
Sleep lost
Baseline sleep
Sleep gain

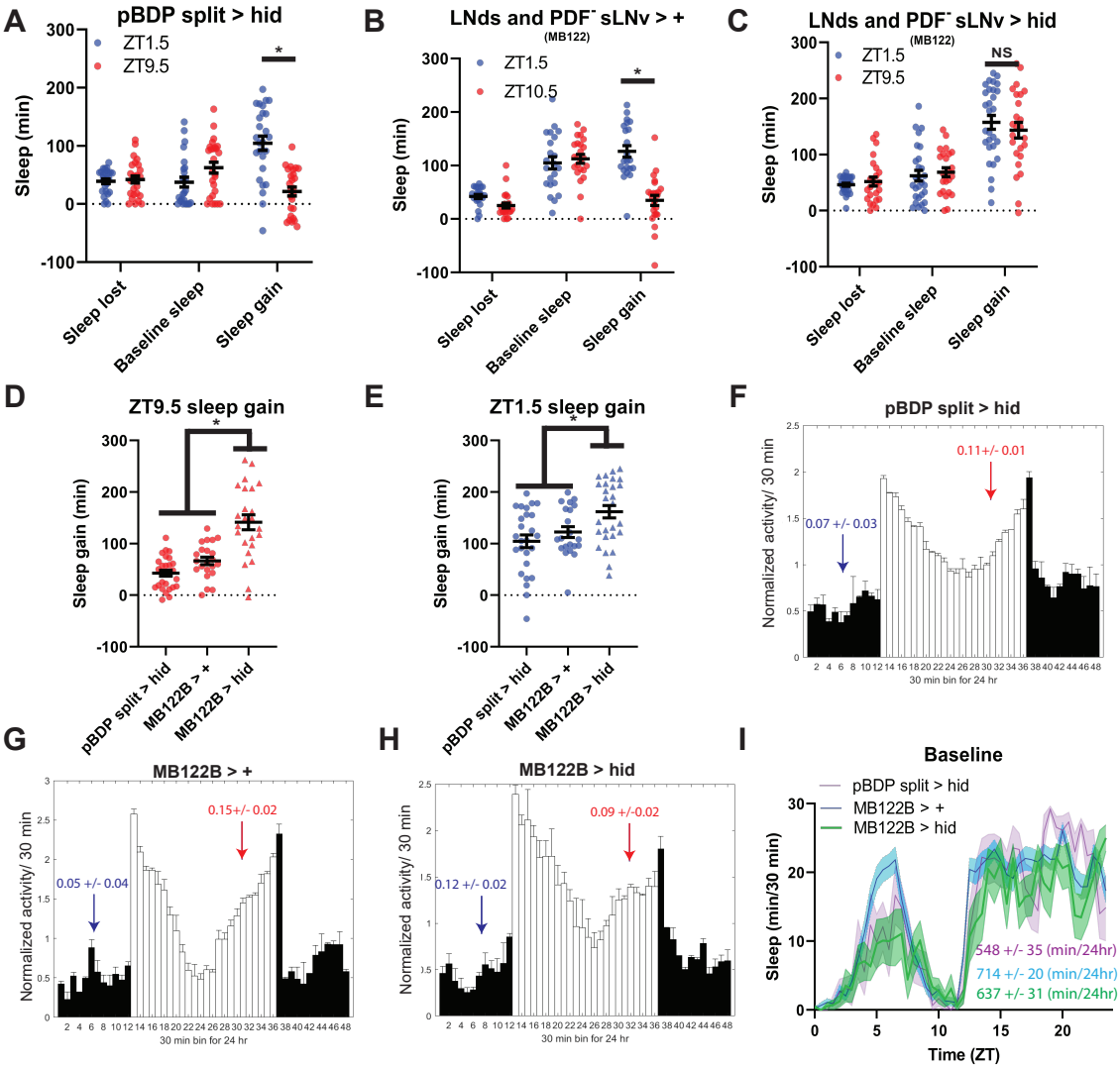
A
pBDP split > hid
ZT1.5
ZT9.5
Sleep (min)
Sleep lost
Baseline sleep
Sleep gain
B
LNds and PDF- sLNv > +
(MB122)
ZT1.5
ZT10.5
C
LNds and PDF- sLNv > hid
(MB122)
ZT1.5
ZT9.5
NS
D
ZT9.5 sleep gain
Sleep gain (min)
pBDP split > hid
MB122B > +
MB122B > hid
E
ZT1.5 sleep gain
F
pBDP split > hid
Normalized activity/ 30 min
0.07 +/- 0.03
0.11+/- 0.01
30 min bin for 24 hr
G
MB122B > +
0.05 +/- 0.04
0.15+/- 0.02
H
MB122B > hid
0.12 +/- 0.02
0.09 +/-0.02
I
Baseline
pBDP split > hid
MB122B > +
MB122B > hid
Sleep (min/30 min)
548 +/- 35 (min/24hr)
714 +/- 20 (min/24hr)
637 +/- 31 (min/24hr)
Time (ZT)

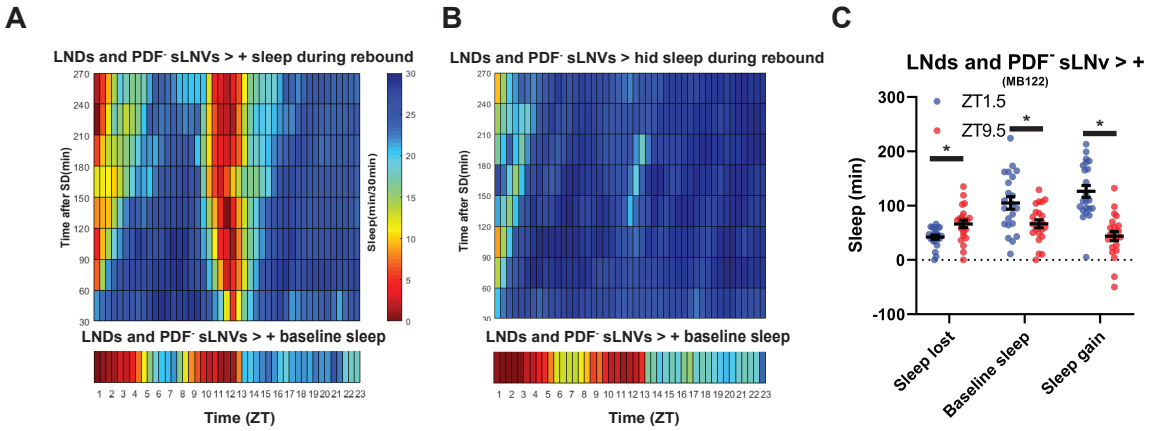
A
LNDs and PDF- sLNVs > + sleep during rebound
Time after SD(min)
Sleep(min/30min)
LNDs and PDF- sLNVs > + baseline sleep
Time (ZT)
B
LNDs and PDF- sLNVs > hid sleep during rebound
Time after SD(min)
LNDs and PDF- sLNVs > + baseline sleep
Time (ZT)
C
LNds and PDF- sLNv > +
(MB122)
ZT1.5
ZT9.5
Sleep (min)
Sleep lost
Baseline sleep
Sleep gain

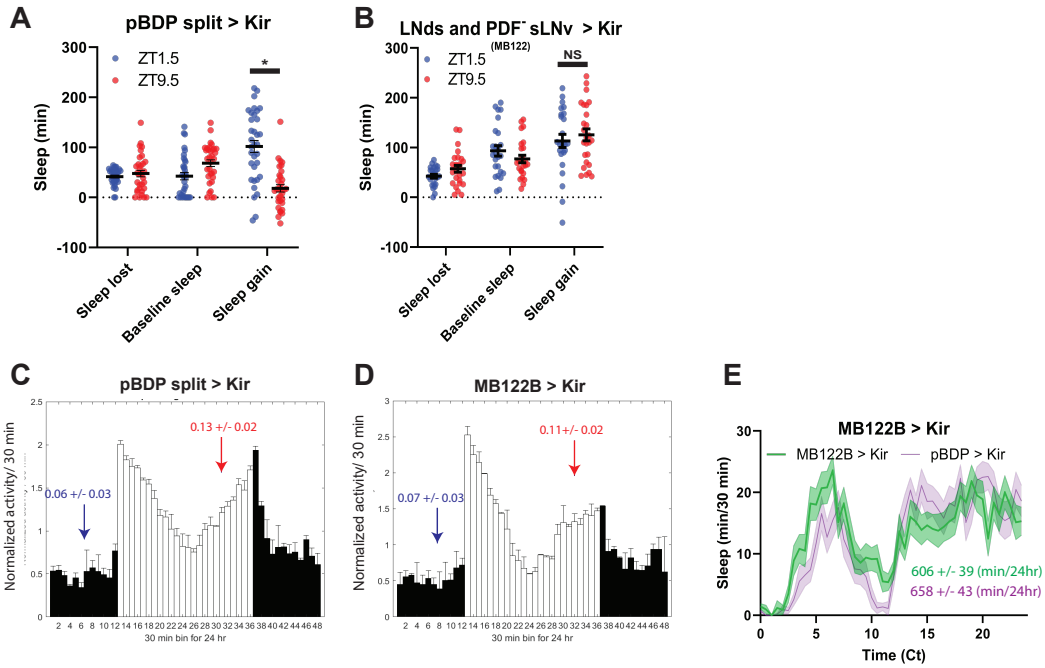
A
pBDP split > Kir
ZT1.5
ZT9.5
Sleep (min)
300
200
100
0
-100
*
Sleep lost
Baseline sleep
Sleep gain
B
LNds and PDF- sLNv > Kir
(MB122)
ZT1.5
ZT9.5
NS
Sleep (min)
Sleep lost
Baseline sleep
Sleep gain
C
pBDP split > Kir
Normalized activity/ 30 min
0.06 +/- 0.03
0.13 +/- 0.02
30 min bin for 24 hr
D
MB122B > Kir
Normalized activity/ 30 min
0.07 +/- 0.03
0.11+/- 0.02
30 min bin for 24 hr
E
MB122B > Kir
MB122B > Kir
pBDP > Kir
Sleep (min/30 min)
606 +/- 39 (min/24hr)
658 +/- 43 (min/24hr)
Time (Ct)

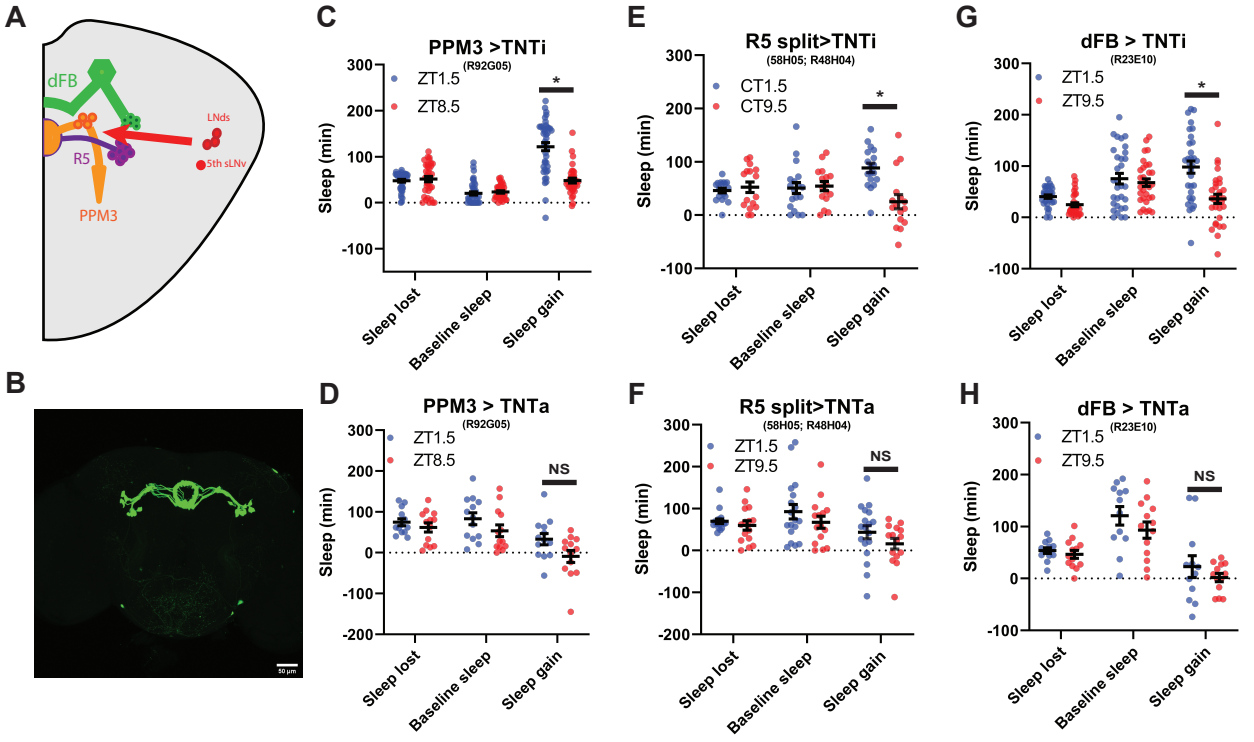
A
dFB
LNds
R5
5th sLNv
PPM3
B
C
PPM3 >TNTi
(R92G05)
ZT1.5
ZT8.5
Sleep (min)
Sleep lost
Baseline sleep
Sleep gain
D
PPM3 > TNTa
(R92G05)
NS
E
R5 split>TNTi
(58H05; R48H04)
CT1.5
CT9.5
F
R5 split>TNTa
(58H05; R48H04)
G
dFB > TNTi
(R23E10)
H
dFB > TNTa
(R23E10)

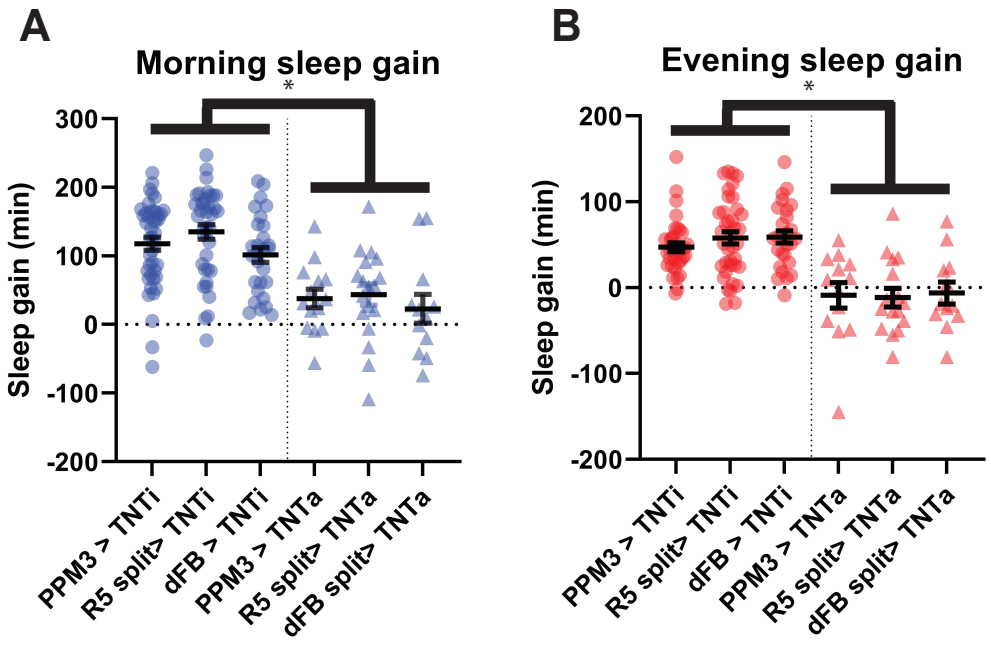
A
Morning sleep gain
*
Sleep gain (min)
300
200
100
0
-100
-200
PPM3 > TNTi
R5 split> TNTi
dFB > TNTi
PPM3 > TNTa
R5 split> TNTa
dFB split> TNTa
B
Evening sleep gain
*
Sleep gain (min)
200
100
0
-100
-200
PPM3 > TNTi
R5 split> TNTi
dFB > TNTi
PPM3 > TNTa
R5 split> TNTa
dFB split> TNTa

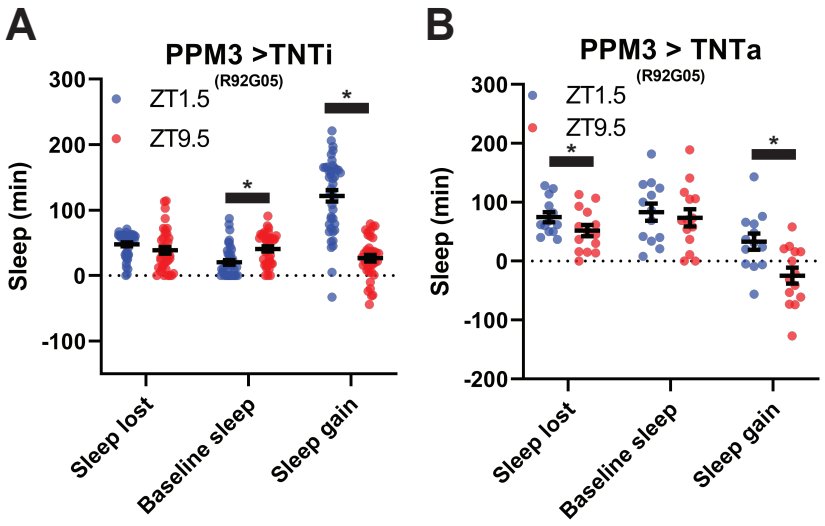
A
PPM3 >TNTi
(R92G05)
ZT1.5
ZT9.5
Sleep (min)
300
200
100
0
-100
*
*
Sleep lost
Baseline sleep
Sleep gain
B
PPM3 > TNTa
(R92G05)
ZT1.5
ZT9.5
Sleep (min)
300
200
100
0
-100
-200
*
*
Sleep lost
Baseline sleep
Sleep gain

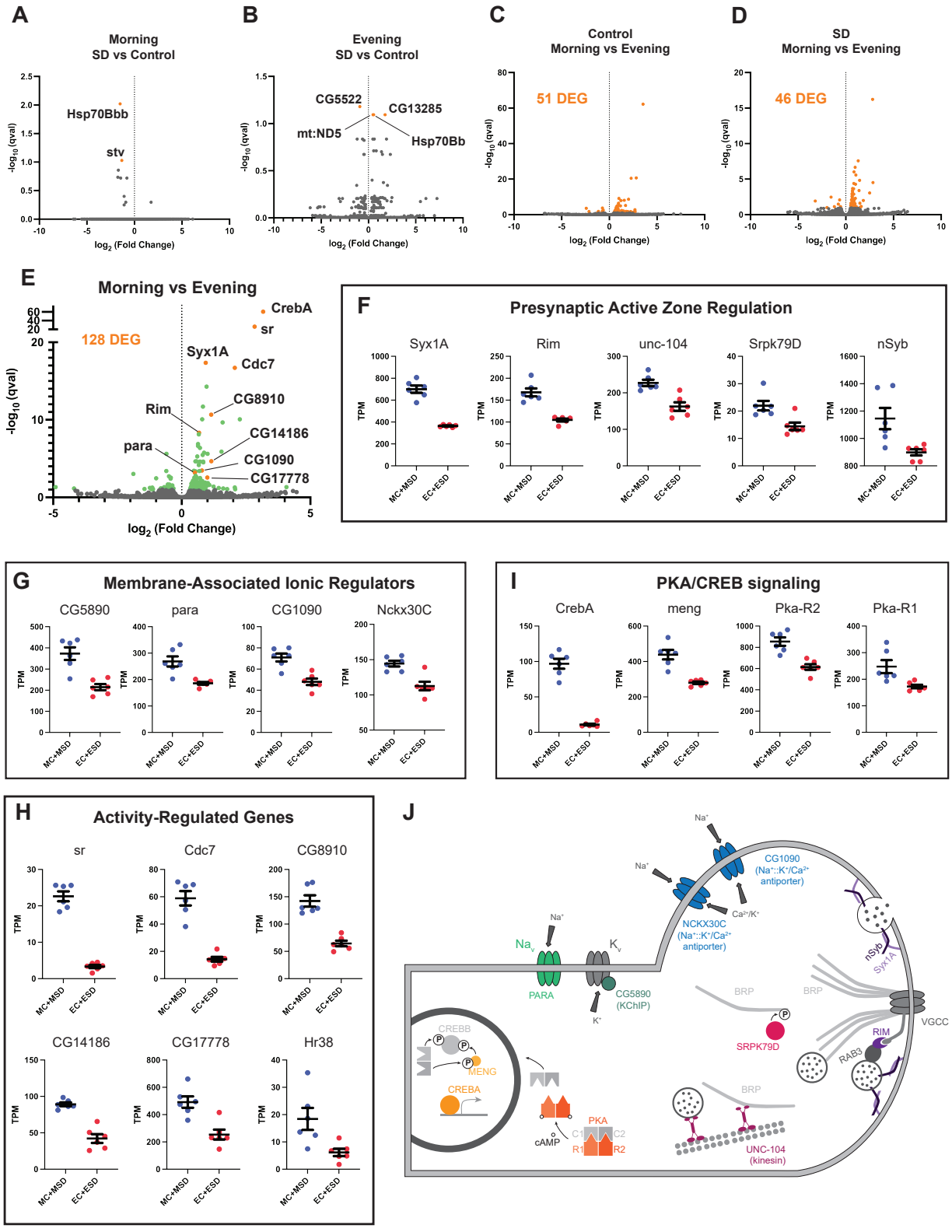
A
Morning
SD vs Control
Hsp70Bbb
stv
B
Evening
SD vs Control
CG5522
CG13285
mt:ND5
Hsp70Bb
C
Control
Morning vs Evening
51 DEG
D
SD
Morning vs Evening
46 DEG
E
Morning vs Evening
128 DEG
CrebA
sr
Syx1A
Cdc7
CG8910
Rim
CG14186
para
CG1090
CG17778
F
Presynaptic Active Zone Regulation
Syx1A
Rim
unc-104
Srpk79D
nSyb
G
Membrane-Associated Ionic Regulators
CG5890
para
CG1090
Nckx30C
I
PKA/CREB signaling
CrebA
meng
Pka-R2
Pka-R1
H
Activity-Regulated Genes
sr
Cdc7
CG8910
CG14186
CG17778
Hr38
J
CG1090
(Na+::K+/Ca2+
antiporter)
NCKX30C
(Na+::K+/Ca2+
antiporter)
PARA
CG5890
(KChIP)
nSyb
Syx1A
BRP
VGCC
RIM
RAB3
SRPK79D
CREBB
MENG
CREBA
cAMP
PKA
UNC-104
(kinesin)

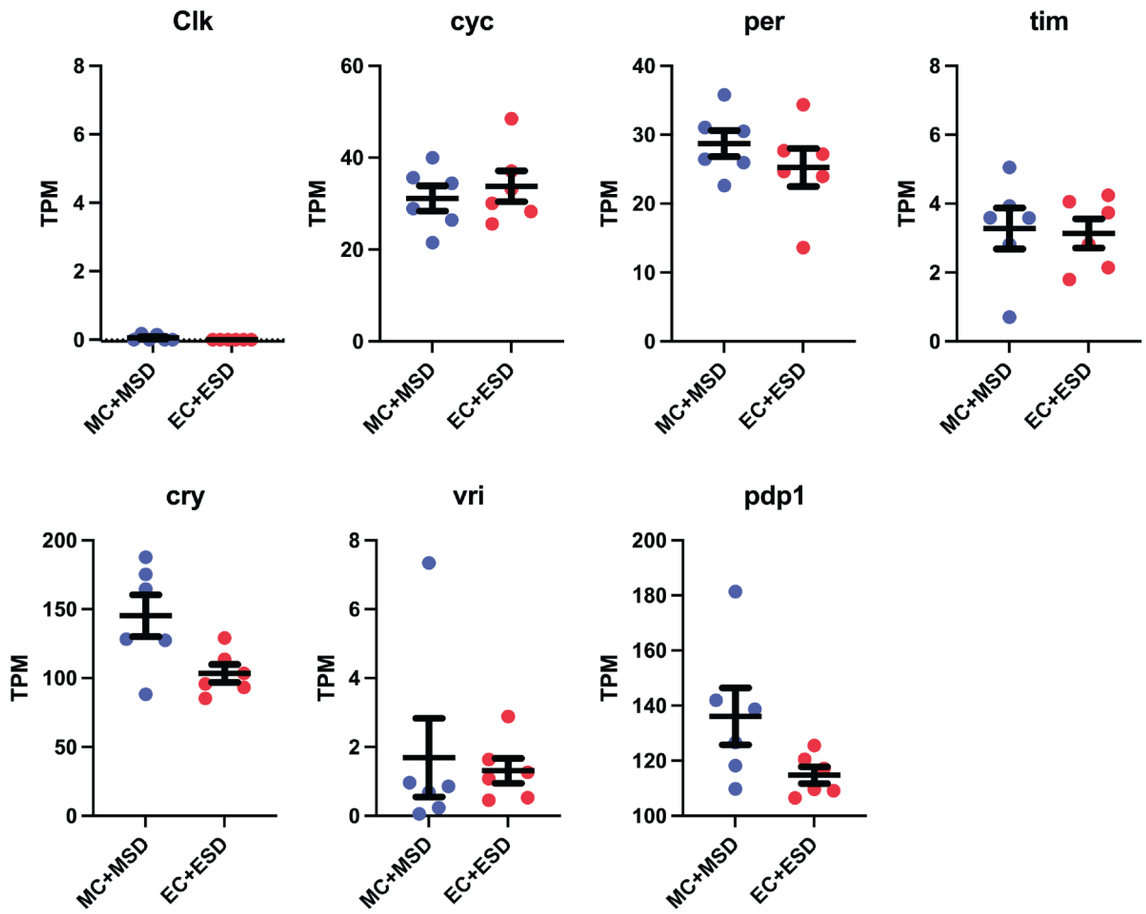
Clk
cyc
per
tim
cry
vri
pdp1
TPM
MC+MSD
EC+ESD

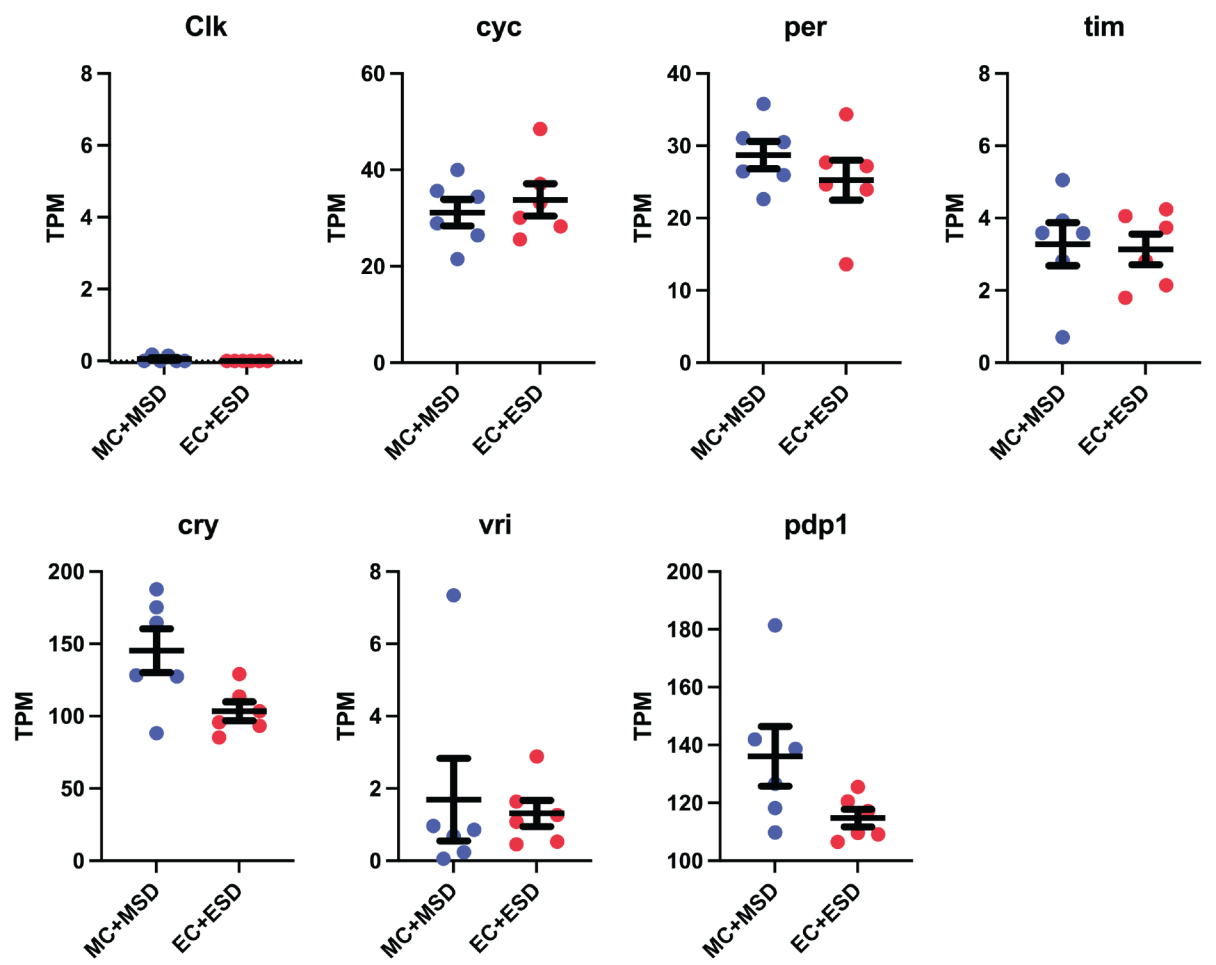
Clk
cyc
per
tim
cry
vri
pdp1
TPM
MC+MSD
EC+ESD

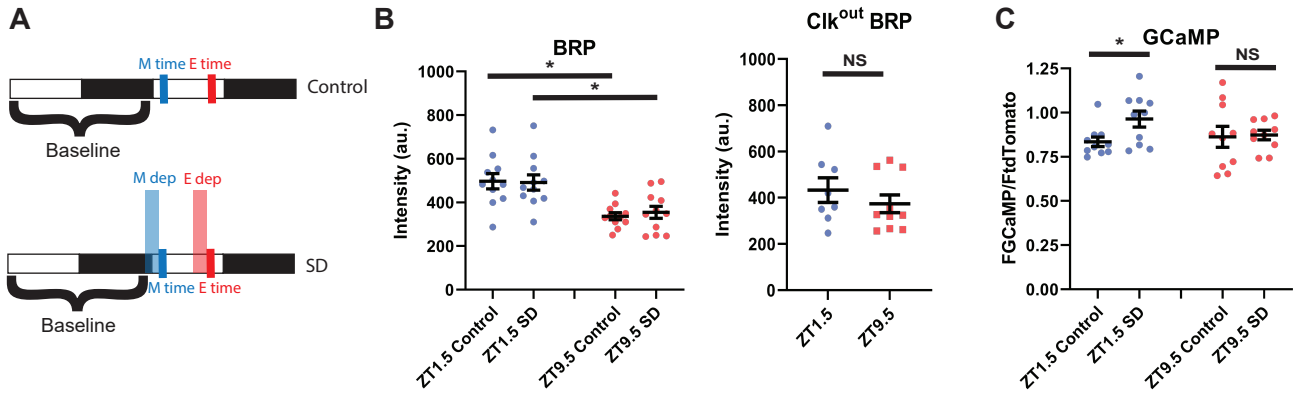
A
M time E time
Control
Baseline
M dep E dep
SD
M time E time
Baseline
B
BRP
Intensity (au.)
1000
800
600
400
200
0
*
*
ZT1.5 Control
ZT1.5 SD
ZT9.5 Control
ZT9.5 SD
Clk^out BRP
NS
ZT1.5
ZT9.5
C
GCaMP
FGCaMP/FtdTomato
1.25
1.00
0.75
0.50
0.25
0.00
*
NS
ZT1.5 Control
ZT1.5 SD
ZT9.5 Control
ZT9.5 SD